Image Based Identification of Endotracheal Path for Robotic Intubation

Thesis submitted for the partial fulfillment of the requirement of the degree of

Master in Control System Engineering

Submitted by

Soumik Dey

Registration Number: 154058 of 2020-2021

Examination Roll Number: M4CTL22008

Under The Guidance of

Dr. Sananda Chatterjee
and
Dr. Sayantan Chakraborty

Electrical Engineering Department

Faculty of Engineering and Technology

Jadavpur University

Kolkata-700032

July, 2022

JADAVPUR UNIVERSITY
Kolkata-700032

Certificate of Recommendation

This is to certify that **Mr. Soumik Dey (002010804008)** has completed his dissertation entitled, **"Image Based Identification of Endotracheal Path for Robotic Intubation"**, under the direct supervision and guidance of **Dr. Sananda Chatterjee** and **Dr. Sayantan Chakraborty**, Electrical Engineering Department, Jadavpur University. We are satisfied with his work, which is being presented for the partial fulfilment of the degree of **Master in Control System Engineering** of Jadavpur University, Kolkata-700032.

……

Dr. Sananda Chatterjee
Visiting Faculty,
Electrical Engineering Department
Jadavpur University, Kolkata-700032

.....

Dr. Sayantan Chakraborty
Assistant Professor,
Electrical Engineering Department
Jadavpur University, Kolkata-700032

.....

Prof. Saswati Mazumdar
Head of the Department,
Electrical Engineering Department,
Jadavpur University, Kolkata-700032

.....

Prof. Chandan Mazumdar
Dean,
Faculty of Engineering and Technology
Jadavpur University, Kolkata-700032

Faculty of Engineering and Technology
JADAVPUR UNIVERSITY
Kolkata-700032

Certificate of Approval

The foregoing thesis entitled "**Image Based Identification of Endotracheal Path for Robotic Intubation**" is hereby approved as a creditable study of an Engineering subject carried out and presented in a manner satisfactory to warrant its acceptance as a pre-requisite to the degree of Master in Control System Engineering for which it has been submitted. It is understood that, by this approval the undersigned does not necessarily endorse or approve any statement made, opinion expressed, or conclusion therein but approve this thesis only for the purpose for which it is submitted.

Final Examination for Evaluation of the Thesis

.....

.....

.....

Signature of Examiners

Declaration of Originality

I hereby declare that this thesis contains a literature survey and original research work by the undersigned candidate, as part of his Master in Control System Engineering curriculum.

All information in this document has been obtained and presented in accordance with academic rules and ethical conduct.

I also declare that, as required by these rules and conduct, I have fully cited and referenced all material and results that are not original to this work.

Name: Soumik Dey

Examination Roll No.: M4CTL22008

Thesis Title: Image Based Identification of Endotracheal Path for Robotic Intubation

Signature:

ACKNOWLEDGEMENT

I sincerely thank my supervisor, Dr. Sananda Chatterjee, Department of Electrical Engineering, Jadavpur University, Kolkata, for her invaluable guidance, suggestions, encouragement, and constant support throughout my thesis work, which helped me in successfully completing it.

I especially thank Dr. Sayantan Chakraborty, Jadavpur University, Kolkata for his innovative discussions, and for sharing his valuable suggestions, ideas and thoughts, which inspired me to do a project in this domain as well as helped me throughout my thesis work.

I am also thankful to my classmate Mr. Arijit Kumar Haldar for his continuous help and support.

Finally, I would like to thank my parents Mr. Shyamal Dey and Mrs. Sonali Dey, my sister Ms. Sneha Dey and my friends for their unconditional support and love.

Soumik Dey

Jadavpur University,

Kolkata

ABSTRACT

Endotracheal intubation, commonly referred to as intubation, is an invasive medical procedure where a flexible plastic catheter is placed into the trachea, usually through the mouth and sometimes through the nose. Intubation is required in critical patients where the airway needs external support to remain open to facilitate general anaesthesia and supply of oxygen or medicine. In most circumstances, managing the patient's airway is pivotal for a safe anaesthetic routine otherwise it may lead to catastrophic implications. According to a recent study, 52% of anaesthesia-related deaths are caused either by respiratory or airway-related problems. A majority of such cases are due to airway injury resulting from excessive force exerted during intubation and injury during airway device insertion or removal.

Several research have been reported to provide technological assistance to the expert to perform a proper and safe intubation. However, most of the works are based on robotic assistance relying on the visual data of the opening of larynx, as seen anatomically, from the top view. There are several instances when the person to be operated has some sort of injury in head, neck or tracheal region and, as a result, the top view of the trachea opening is cluttered with blood and mucus. Thus, it becomes quite unpredictable when it comes to inserting the tube. Hence, in majority of the cases the movement of the tube inside the trachea is purely based on the intuition of the doctor or the anaesthesiologist performing the task.

In order to address this issue, the present work traces the pathway of the endotracheal region based on the side view of the neck captured using a CT image, so that we can get a clear detection of the endotracheal path. To this end, a machine vision based algorithm is developed which approximates the endotracheal path as a concatenation of standard conic section arcs. The algorithm is studied for critical cases like patients with head and neck injury and paediatric cases. Such a detection of endotracheal path helps in (i) calculating approximate curvature, diameter and length of the tracheal tube to be inserted and (ii) estimating a safe entrance mechanism for a continuum robot to execute endotracheal intubation with a low chance of damage.

Keywords: Endotracheal intubation, Machine Vision, Conic Section, Path Detection.

Contents

List of Figures

List of Abbreviations

EI	Endotracheal Intubation
ETT	Endotracheal Tube
TT	Tracheal tube
TI	Tracheal Intubation
EMS	Emergency Medical Service
METI	Magnetic Endotracheal Intubation
CETI	Classic Endotracheal Intubation
MGI	Magnetically Guided Intubation
ITD	Internal Tracheal Diameter
KIS	Kepler Intubation System
RGB	Red Green Blue
CMYK	Cyan Magenta Yellow Key
HSV	Hue Saturation Value

Chapter 1

Introduction

1.1. HISTORY AND BACKGROUND OF ENDOTRACHEAL INTUBATION

Endotracheal intubation, commonly referred to as intubation, is an invasive medical procedure where a flexible plastic catheter is placed into the trachea i.e. windpipe usually through the mouth and sometimes through the nose [1]. Intubation is required in critical patients where the airway needs external support to remain open so that general anaesthesia, oxygen, or medicine can be provided. Sometimes intubation is needed to support breathing in people with emphysema, pneumonia, heart failure, severe trauma, or collapsed lung. Moreover, intubation prevents fluid from entering the lungs due to stroke, overdose, or massive bleeding from the stomach or oesophagus (feeding tube) and occasionally helps in removing blockage from the airway [2].

For years, tracheotomy , which is a surgical procedure performed by making an incision or cut on the front side of the neck which creates a direct path for airway in the trachea. Although this procedure was very risky, it was considered the most reliable method of tracheal intubation. Ancient Hindu records from circa 2000 BC and Egyptian writings from around 1500 BC contain the earliest descriptions of tracheostomies [3]. Since then, other reports in both animals and people have demonstrated the value of tracheostomy surgery in saving lives. In 1543, Vesalius recorded the first animal tracheal intubation. Afterwards, Trousseau noted 200 diphtheria victims who were kept alive by tracheostomies. Later, Trendelenburg from Germany performed the first endotracheal anaesthesia on a human patient in the early 1870s. The first elective endotracheal intubation for anaesthesia was documented by Macewen in

1878. He protected the trachea from leakage of blood and debris by packing the hypopharynx. Later, cocaine was given as a local anaesthetic by Rosenberg and Kuhn to stifle the cough reflex during intubation.

During the First World War, intubation and tracheostomies were often utilised. Tracheal intubation has benefits, which Magill (1888-1986) observed. Additionally, because of his work, anaesthesia is now a separate field of study. Jackson created the first anaesthetic laryngoscope in 1913, and Magill, Miller, and Macintosh improved on it. Endotracheal intubation became customary in major abdominal and other surgeries in 1942 after the introduction of the muscle relaxant curare for use during general anaesthesia. In the 20th century endotracheal intubation is a crucial part of the practices of anaesthesia, critical care medicine, trauma treatment, emergency medicine support, breathing in people with pneumonia, emphysema, heart failure, collapsed lung, gastroenterology, pulmonology, and surgery. Now in the 21st century, like any other medical procedure the tracheal intubation has also been modernised as an effect of the "digital revolution". Video laryngoscopes are developed with the help of CMOS active pixel sensor technology that generates a view of the glottis which assist in intubation inside the trachea.

1.2. DIGITAL IMAGE PROCESSING AND ITS USE IN MEDICAL FIELD

The alteration of digital photographs using a digital computer is known as "digital image processing." Although it is a branch of signals and systems, it specialises in visuals. The goal of digital image processing is to create a computer system that can manipulate images. A digital image is used as the system's input, which is processed by the system utilising effective algorithms to produce an image. Any method created for one dimension can be applied to the rows first, then the columns, of the matrix that represents this digital image. The image of molecular or whole organs, organ systems, and body parts are depicted in the biomedical images. The technology of image processing is extremely important for comprehending and extracting information from these images. Medical imaging is the process of creating a visual image of the interior segments or interior body parts for clinical examination, medical intervention, and a visual representation of the operation of a few organs or tissues. With the aid of digital image processing techniques in the medical industry, digital imaging techniques have made it feasible for doctors to quickly detect disorders.

Different medical imaging techniques identify different physical signals obtained from a human body under investigation and construct related images. Particular techniques are used for particular imaging system [4]. Examples of some medical diagnostic imaging techniques are projection radiography and x-ray computed tomography (CT) where x-rays are transmitted across the patient's body and obtains the image; digital subtraction angiography (DSA) which subtracts "pre-contrast" and "post-contrast" images and in turn produces enhanced images of the blood vessels; images of the soft tissue in the breast are captured using Mammography; delivery of Nuclear medicine is inspected by capturing the emission of gamma rays initiating from the radiotracers injected into the body; planar scintigraphy and emission computed tomography (SPECT and PET) are used; The reflection of ultrasonic waves within the body are captured using Ultrasound imaging; Magnetic resonance imaging (MRI) is used to capture the precession of spin systems in a large magnetic field; multi-modal images are registered with the help of functional MRI (fMRI).

Some of these imaging techniques are based on ionizing radiation, where the atoms and molecules within the body are ionized using sufficiently energized radiation, and others are based on non-ionizing radiation. Examples of ionizing radiation in medical imaging are x-rays and γ-rays, both of which need to be used carefully to avoid causing serious damage to the patient's body under diagnosis. Non-ionizing radiation, on the other hand, are costlier and the risks associated with their use are considered to be very low and does not have the potential to damage the body directly. Examples of such radiation are radio frequency waves, and ultrasound, i.e. high-frequency sound.

In this thesis computed tomography (CT) images are used for detecting the shape of the trachea for robotic endotracheal intubation. Here, x-rays is used for illustrating anatomical features and has enabled tomographic reconstruction of images.

1.3. PROCESS OF ENDOTRACHEAL INTUBATION

Endotracheal Intubation (EI) is frequently a life-saving treatment used on unconscious or unable-to-breathe patients. EI keeps the airway open and aids in suffocating prevention.

To keep the airway open during endotracheal intubation, a plastic tube known as an endotracheal tube (ETT) is inserted into the trachea. By allowing an external source to take over the physiology and energy of breathing, as well as by safeguarding their lungs to prevent

the development of pulmonary disease, this method saves individuals who are experiencing respiratory distress or failure [1]. Modern TIs involve raising the patient's jaw with a laryngoscope while inserting a ETT into their trachea. Because it gives a clear view of the glottis, the trachea's entry, this method is known as "direct-laryngoscopy". Asphyxia, hypoxia, and pulmonary aspiration can cause serious morbidity and fatality if EI is not performed in time or ETT is performed incorrectly [2]. In EMS scenarios where EI is carried out under challenging and demanding conditions, these casualties happen more frequently [3].

Fig 1.1: (left) Intubation performed by medical expert [11], (right) instruments used for endotracheal intubation [12]

A blade, a laryngoscope, and an ETT are required for traditional intubation. The operator pushes the blade into the mouth while pushing the tongue aside as they stand behind the supine patient to determine the location of the glottis. The glottis, or the area between the vocal cords, is exposed as the soft epiglottis is forced upward by the blade's tip. The ETT is then inserted into the trachea or windpipe through the vocal cords. However, this strategy may fail if it is difficult to perceive the glottis, which problem is a direct outcome of the previously mentioned causes. Many technologically advanced gadgets have been created and employed in clinical settings to solve this problem. One of the most common technology-integrated methods is video laryngoscopy, which makes use of a blade with a tiny camera and light source at its tip to allow the patient to see the epiglottis on a screen attached to the camera [5],[6]. The process of manual EI requires highly specialized medical experts. Image of the manual insertion and the instruments used in the process are shown in Fig. 1.1.

1.4. MOTIVATION

In most circumstances, managing the patient's airway is a vital issue for a safe anaesthetic routine, but it has been known for a very long time that problems with airway management can have catastrophic implications. Fifty two percent of anaesthesia-related deaths, according to a recent study report, are caused either by respiratory or airway-related problems. Direct or indirect airway injury can result from general anaesthesia. Excessive force utilised during airway instrumentation results in direct harm, as does injury during airway device insertion or removal. Inadequate oxygenation, ventilation, or airway protection are examples of indirect harm, and these ailments may coexist with respiratory issues. It is anticipated that acute airway blockage will be a medical emergency with a high risk of morbidity and fatality.

Giving untrained physicians robotic help to perform EI is intriguing because it may be able to overcome their limitations owing to their lack of experience. In severe situations requiring in-hospital EI, it might also enhance the performance of seasoned doctors. By identifying important anatomical features of the patient's trachea, a robotic assistant would actively guide the ETT into the trachea through the glottis entrance. A lot of work has been done previously based on robotic assistance but all the work that had been done till now is based on the opening of the larynx as seen from the top view anatomically. As a result of which it becomes quite unpredictable when it comes to inserting the tube, because there are several instances when the person to be operated has some sort of injury like head injury, neck injury, tracheal injury and much more. In such cases, the top view of the trachea opening is cluttered with blood and mucus and the vision, even if when using camera for video laryngoscopes, is lost. Hence, the movement of the robot inside the tracheal tube, as a result, is purely based on the intuition of the doctor or the anaesthesiologist performing the task.

So, in this work we try to trace the pathway of the endotracheal region considering the side view of the neck captured using a CT image, so that we can get a clear detection of the endotracheal path and also deduce some mathematical relations which would enable us to ensure near about exact curvature, diameter and length of the tracheal tube to be inserted.

1.5. OUTLINE OF THESIS

In chapter 1, a quick summary of the digital image processing and its use in medical field has been discussed along with the history of endotracheal intubation and the technicalities involved in the procedure.

In chapter 2, a thorough literature survey is done on the methods used in the process of endotracheal intubation. Emphasis on the traditional intubation techniques has been given along with all the corresponding and necessary research works that had been carried out in the past few years. A brief literature survey on the most recent approaches using artificial intelligence, machine learning and robotics has also been discussed.

In chapter 3, the steps for the detection of the intubation path have been discussed in details. Here, we will find the extensive use of image processing techniques. To establish a broader area of expertise we have considered a few case studies in which we have taken into account the detection of the intubation path of injured persons.

In chapter 4, the development steps of the Graphical User Interface are presented. The application of the Hough transforms with suitable conditions for finding the conic sections such as circles and ellipse are discussed. Methods applied to mark the start and end points on the circle and finding the arc of relevance is also reported in this chapter.

In chapter 5, the results obtained from the algorithm developed are presented for four cases (i) normal endotracheal airway, (ii) patient with head injury, (iii) patient with neck injury, (iv) paediatric airway. The results follow a detailed discussion on all the cases.

Chapter 6, points out two major applications of the developed algorithm for detection of endotracheal path. This detection algorithm may be employed to calculate approximate curvature, diameter and length of the soft/flexible tracheal tube used in passive intubation. Another application of the algorithm could be estimating a safe entrance mechanism for a continuum robot to execute active robotic endotracheal intubation. Finally, it concludes the whole thesis work, and also provides direction for future research in this domain.

Chapter 2

Literature Survey

2.1 INTRODUCTION

Endotracheal Intubation is a complex medical procedure which involves the insertion of a tube through the mouth of the patient down into the trachea. The procedure is often executed with the help of an instrument called *laryngoscope*, which allows the operator to view the glottis and the vocal cords to facilitate the operation. It involves a complex psychomotor skill and in many clinical situations it proves to be a potentially lifesaving procedure. It has been reported in literatures that if the airway is secured early using tracheal intubation then it yields improved outcome especially for critically ill and injured patients.

Difficulties involved in tracheal intubation procedure are one of the major causes of the anaesthesia related injuries, which may lead to potential life threatening complications. Anticipation and proper detection of the airway in the pre-operative stage is, therefore, crucial for the safety of the patient.

In the recent past a number of research works have been carried out to facilitate a smooth, painless and error-free endotracheal intubation. In several of those cases the techniques of image processing have been utilised. Some of the important works are presented next.

2.2 TRADITIONAL METHODS OF ENDOTRACHEAL INTUBATION

Endotracheal Intubation (EI) is the procedure used by Emergency Medical Services (EMS) to secure a patient's airway when they require respiratory assistance while under general

anaesthesia [1]. A Tracheal Tube (TT) is inserted into the patient's trachea as the patient's jaw is raised using modern EI techniques. This procedure is called "*direct-laryngoscopy*" because it allows a clear view of the glottis, which serves as the trachea's entrance. If EI is postponed or TT is introduced inappropriately, asphyxia, hypoxia, and pulmonary aspiration can result in significant morbidity and fatality [2]. For classic intubation, a blade, a laryngoscope, and an ETT are needed. To locate the glottis, the operator stands behind the reclining patient and puts the blade into the mouth while pushing the tongue aside. The soft epiglottis is propelled upward by the blade's tip, exposing the glottis, or the space between the vocal cords. The tube is then inserted via the vocal chords into the trachea. However, this strategy may fail if it is difficult to perceive the glottis, which problem is a direct outcome of the previously mentioned causes. To address this issue, a variety of cutting-edge devices have been developed and used in clinical settings. Video laryngoscopy, which uses a blade with a tiny camera and light source at its tip to let the patient see the epiglottis on a screen linked to the camera, is one of the most popular technology-integrated techniques.

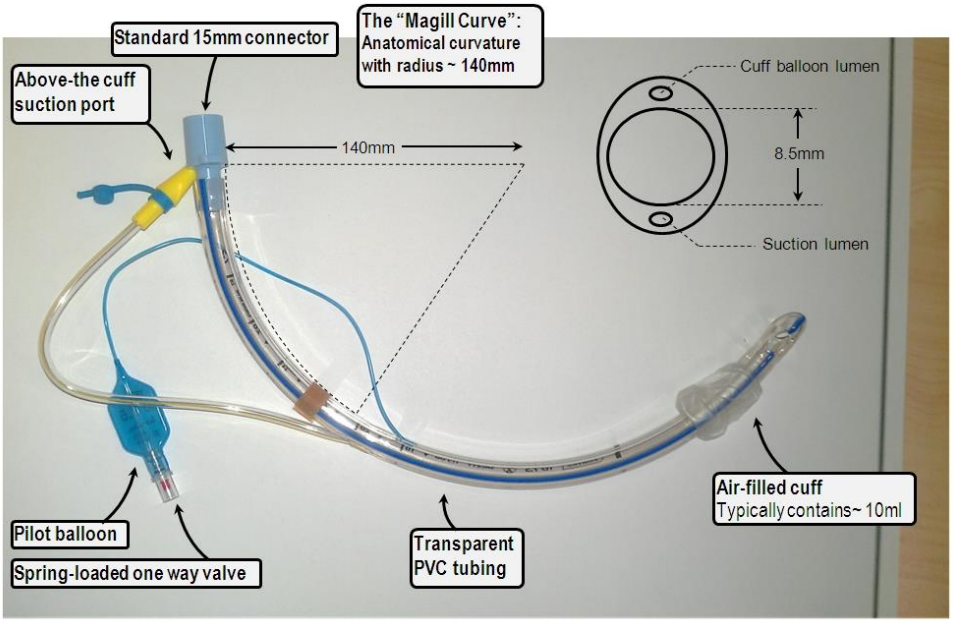

Fig 2.1: A typical tracheal tube [13]

The work of [6] examined 768 patients with major complications, sometimes even life-threatening ones, to demonstrate the application of a video laryngoscope. In another literature [7] a camera is being inserted into the tip of the tracheal tube during tracheal intubation carried out on patients and manikins. This arrangement was employed especially to enable continuous visualisation of the trachea and carina during surgery and bronchial blocker insertion without

the use of fibreoptic bronchoscopy. Figure 2.1 shows the arrangement where camera is attached at the end of the tube.

Fig 2.2: Close-up of the camera in the tip of the tracheal tube [16]

2.3 DIFFERENT TYPES OF PROBLEMS RELATED TO DIFFICULT AIRWAYS

A problematic airway is a clinical scenario in which a healthcare professional finds it difficult to employ one or more of the well accepted airway management techniques. Even for professionals with a wealth of experience and knowledge in this field faces trouble in such situations even with the normally used devices like the laryngoscope supraglottic devices. Common and otherwise useful surgical instruments seem to fall short of expectations. The degree of such difficulty in handling the situation using any other technique varies widely and is influenced by a number of factors including the patients characteristics, medical and surgical history, previous instances of any type of injuries suffered and most importantly on the patients current condition and the vital signs.

In the work of [15], a case study of a patient with a substantial three-column cervical spine injury is discussed. This damage was initially overlooked and discovered upon revaluation two weeks after the initial incident. It was discovered that the antero-superior

osteophyte of the C7 body had an acute fracture (as shown in Figure 2.3 (a)). Additionally, the cervical facet at C6/7 had an opening, as can be seen in Figure 2.3 (b).

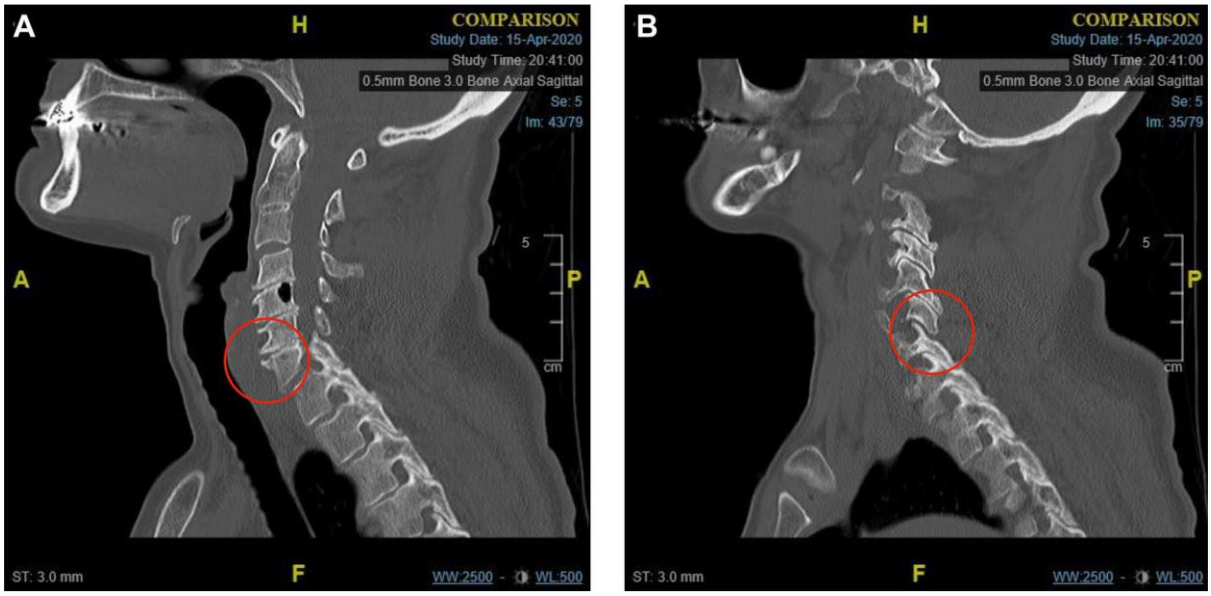

Figure 2.3: (a) A para-midline sagittal CT scan of the cervical spine taken at the time of the patient's initial presentation reveals a fracture of the C7's antero-superior osteophyte (depicted by a circle), and (b) A para-midline sagittal CT scan of the cervical spine taken at the time of the patient's initial presentation reveals that the C6/C7 facet joint is opening (a circle is used to illustrate this) [15]

In such cases of injury to the spine, the neck region including the endotracheal cavity gets deformed to a large extent. Then it becomes quite problematic for the medical experts to perform the intubation. This is due to fact that the professional performing the task can only get an idea of the endotracheal tract but the insertion of the tube is purely based on his intuition.

So during an emergency when the intubation has to performed urgently because of the serious condition of the patient, inserting the tube through the deformed passage can lead to choking or further injury to the tract making the situation even more tense and serious.

Paper [17] discusses about the abnormalities and disorders related to digestive tract of paediatrics. In the paediatric population, there are a number of significant aerodigestive tract anomalies that call for a precise imaging evaluation and diagnosis to guide the right care and reduce potential problems. The paediatric and adult airways differ significantly anatomically in a number of significant ways. Infants have a large occiput, which causes the neck to bend somewhat when the head is flat, kinking the airway. Infants have a narrow, sigma-shaped epiglottis, but adults have a larger, U-shaped epiglottis. Children's vocal chords are also

anteriorly angulated. The arrangement of the epiglottis and the relative anterior angulation of the vocal cords makes it even more difficult to reach the glottic opening to create an airway during endotracheal intubation. The difference in the airway between a child and an adult is shown as shown in Figure 2.4.

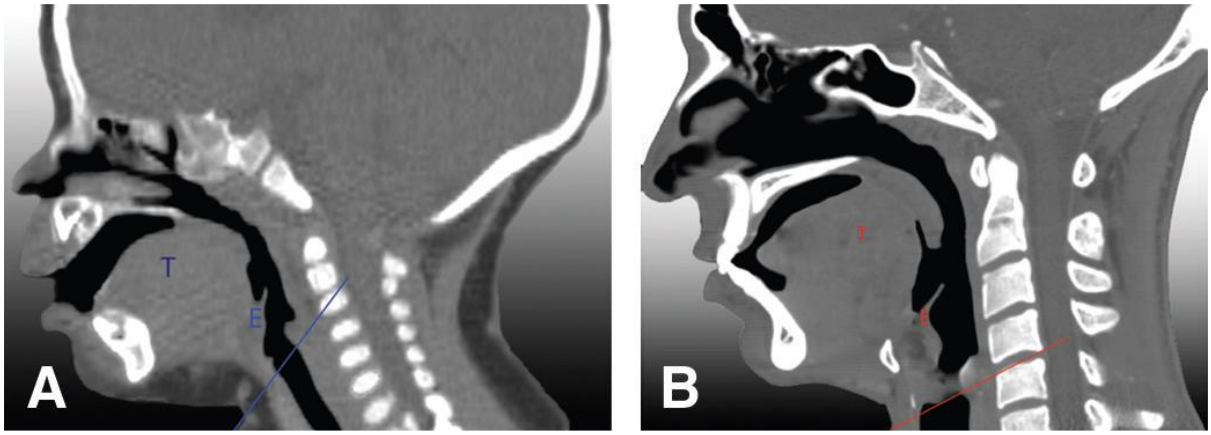

Fig 2.4: differences between the airways shown on lateral radiography in children and adults. The trachea starts higher at the C2-C3 level in the paediatric airway (A), but in adults, it starts lower at the C4-C5 level (B). Just below the cricoid cartilage is where the trachea starts. Additionally, the tongue (T) occupies a larger portion of the oral cavity in youngsters and the epiglottis (E) is pointed away from the axis of the trachea [17]

2.4 SOME ADVANCED INTUBATION TECHNIQUES FOR DIFFICULT AIRWAYS

Advanced airway management is an ingenious way of managing the airway of a patient which is very different from the basic airway management. In basic airway management medical expertise is not required, but in advanced airway management better training, medical expertise, use of medicines and modern medical equipments are required. It includes a variety of procedures used to open or patent an airway - a direct line from the lungs of a patient to the outside world.

The task is achieved by removing or avoiding airway blockages. A number of different factors, such as the patient's own tongue, or other anatomical airway components, foreign

objects, excessive volumes of blood and body fluids, or aspiration of food particles, can obstruct the airway.

Advanced airway management requires the use of medical equipment and advanced training, contrary to the basic airway management techniques like the head tilt/chin lift or jaw-thrust procedure.

The work of paper [14] by J.M. Huitink et al. presented a technique which involves inserting a fibrescope into the throat following topical anaesthesia. This method is suitable for tracheal intubation in patients with a known difficulty in the airway, such as those with head or neck cancer. It may become extremely difficult for the anaesthesiologist to follow the endotracheal channel due to the size and location of the tumour, as well as anatomical changes brought on by extensive reconstructive surgery, chemotherapy, or radiotherapy in the past. In this method, a unique suction catheter is inserted into the airway through the fiberscope's suction channel to monitor the amount of carbon dioxide in the air. The detection of the CO_2 gradient was used to confirm the position of the TT into the trachea.

Fig 2.5: A fiberscope with airway suction catheter connected to oxygen (O_2), filter and gas sample line (CO_2) [14]

In [20], authors Sedat Bilge et al., designed a stylet, specifically for the study, which is modified with an iron ball affixed to the tip and a neodymium magnet. The objective was to guide, with the help of the modified stylet and the magnetic force of the neodymium magnet, the endotracheal tube into the trachea at the level of the thyroid and cricoid cartilages on the

manikin. A comparison of the success rate, completion time, and degree of difficulty of two procedures: Magnetic Endotracheal Intubation (METI) and Classical ETI (CETI) illustrates that both the processes are highly successful.

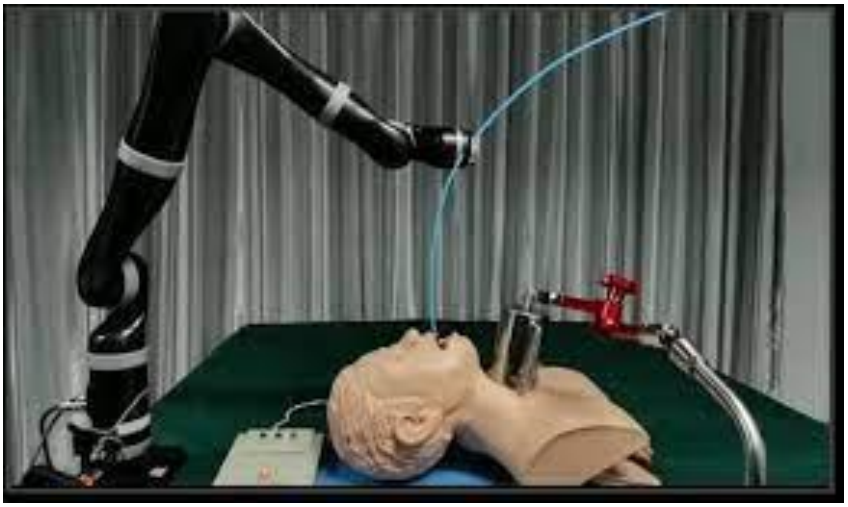

Fig 2.6: magnetically guided orotracheal intubation [19]

2.5 USE OF ROBOTIC DEVICES TO AUTOMATE INTUBATION

Tracheal intubation when done manually depends on the operator's skill, knowledge and experience to identify important anatomical characteristics such the glottis, and direct the TT into the trachea.

Giving untrained personnel a robotic help to perform EI is intriguing as it may help them to overcome their limitations owing to lack of experience. In severe situations requiring in-hospital EI, a robotic aid might also enhance the performance of seasoned doctors. By identifying important anatomical features of the patient's upper airway, a robotic assistant would actively guide the tracheal tube towards the glottis entrance and into the trachea.

This will lead to a step closer to the level of accuracy and efficiency that the medical industry must unavoidably achieve. Automated intubation will lead to breakthroughs in a variety of emergency scenarios, including those involving patients with problematic airways, emergency room staff who must divert their attention to more critical circumstances, or when a difficult airway is anticipated. As is presently common with the automated defibrillator used in cardiac arrest, we also foresee a completely new setting in which people without medical training will be able to care for persons who are experiencing respiratory arrest.

Thereby, Robotic assisted EI would pave the way for a safer and more efficient airway management by facilitating EIs.

In [21] Hemmerling et al. developed the Kepler Intubation System that consists of a robotic arm, remotely controlled via a joystick by the operator, that manipulates the video-laryngoscope. Robotic intubation was successful in 11 out of 12 patients. This system, however, does not include any automation feature, rather it fully relies on a visual recognition of the airway followed by a manual steering by the operator as shown in Figure 2.7.

A video laryngoscope robotic arm

A joystick

Fig. 2.7: The Kepler intubation system [21]

Fig. 2.8: Lateral view of the setup of the KIS [21]

In [22], the authors Quentin Boehler et al created a device called REALITI, or Robotic Endoscope Automated through Laryngeal Imaging for Tracheal Intubation. In order to guide the TT into proper position, the robot moves towards the anatomical features which are detected automatically. The feature identification helps to control the endoscope visually. This prototype has been used to successfully introduce the objects normally and automatically into the endotracheal region. In order to give a reliable detection, a detector based on Haar Cascade Classifiers is particularly trained to recognise four important anatomical features in an airway management training manikin.

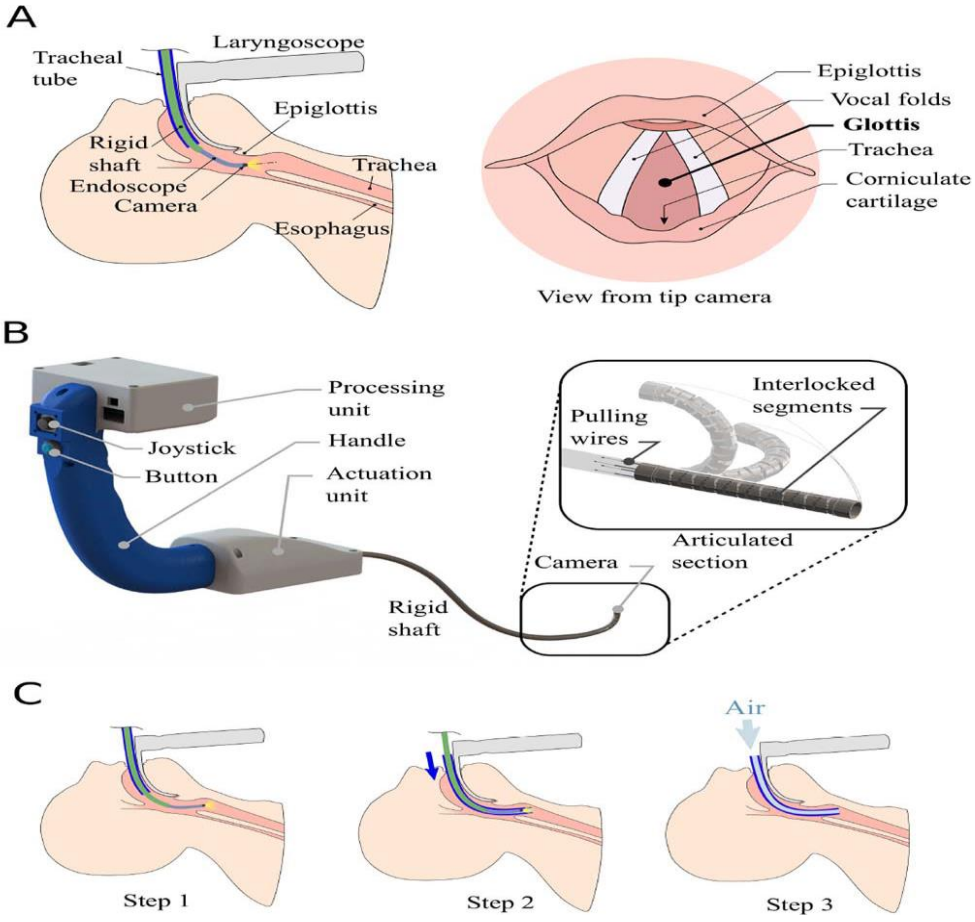

Fig. 2.9: Tracheal intubation assisted by robots. A: Prepare the video-endoscope for larynx navigation, B: The REALITI device; C: The REALITI intubation technique [22]

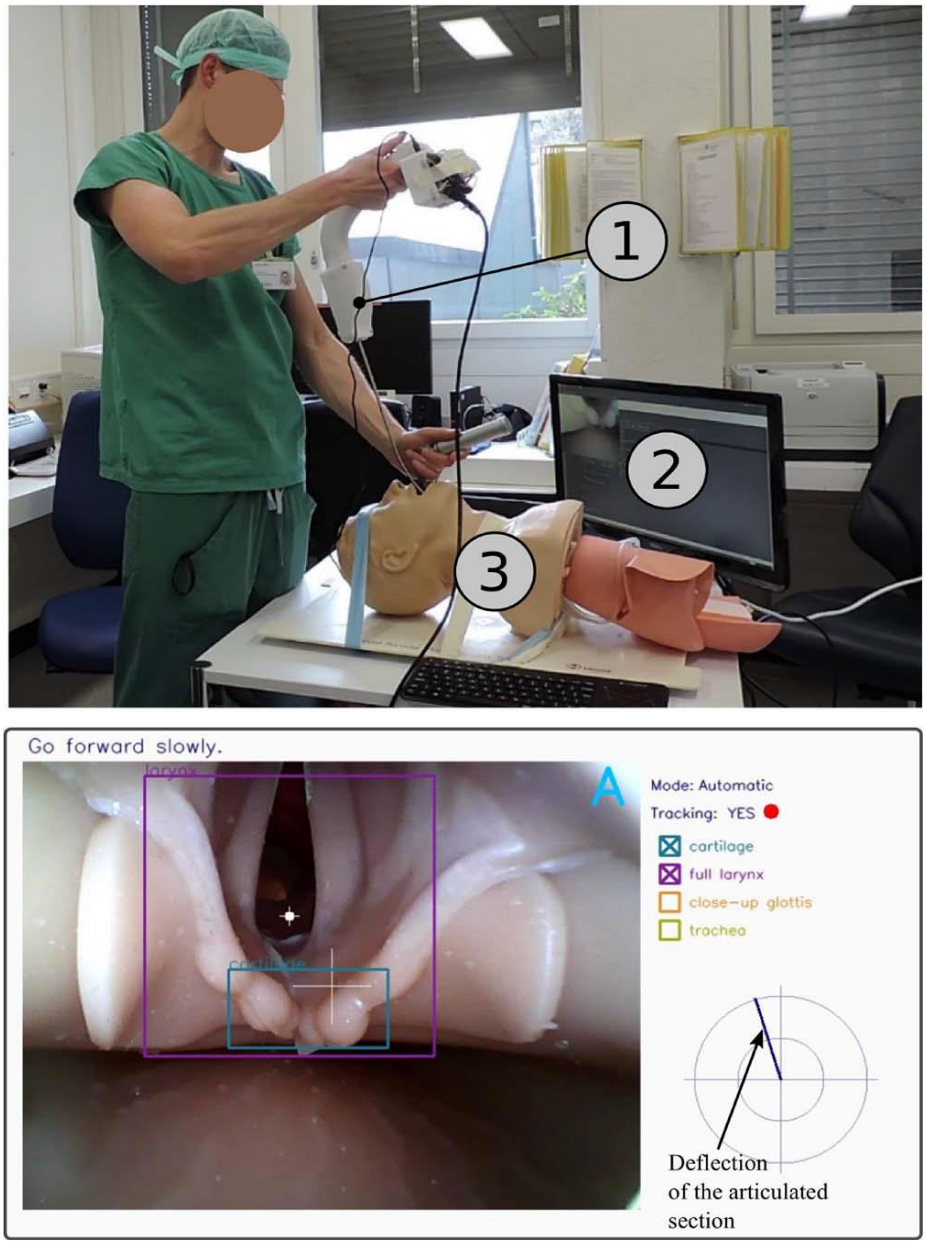

Fig. 2.10: Get the training manikin ready for the tests. Top: test setup featuring the REALITI prototype, an external display, and a training manikin (3). The user interface is presented at the bottom of the external monitor [22]

Chapter 3

Detection of Intubation Path

3.1 INTRODUCTION

There are various steps involved in the detection of integration path of the endotracheal region. At first, one needs to choose suitable images so that one can proceed further with minimum pre-processing techniques to be applied. For this reason here I have chosen computed tomographic (CT) images as the input images. CT scans use X ray radiations, they are less expensive than MRI but still provide good quality images. CT images are relatively less noisy as compared to MRI images even though MRI provides much clearer images that of tissues organs but in our case we do not need so much detailed images of the tissues because then it becomes difficult to distinguish between the areas of our interest and the unimportant part especially when we proceed to contrast stretching techniques and thresholding in later stages. The various stages of image processing techniques applied in this work are discussed below:

3.2 CONTRAST STRETCHING

By simply extending the range of intensity values a picture includes to a wider spectrum of desired values using the whole range of pixels, contrast stretching is a straightforward image enhancement technique that improves the contrast in an image. This method of contrast stretching will not only improve the quality of image but also remove appreciable amount of noise from it. Also in certain regions, there are some noisy and unclear edges which need to be clearly demarcated from our next processes. The general formula for image contrast stretching is given by:

$$c = (a - a_{min}) \frac{(i_{max} - i_{min})}{(a_{max} - a_{min})} + i_{min}$$

For, $i_{min} = 0 \; and \; i_{max} = 255$;

$$c = 255 \times \frac{(a - a_{\min})}{(a_{max} - a_{\min})}$$

where,

a = current pixel intensity value

a_{min} = minimum intensity value present in the whole image

a_{max} = maximum intensity value present in the whole image

Digital radiographs, often known as digital x-ray images, are produced using x-ray cameras, which have an array of x-ray detectors as their main component. The quality of the x-ray beam and the item being scanned affect how much x-ray illumination the detectors receive, which affects how much charge they gather (which shows up as a higher pixel intensity). Because a dense item prevents more x-rays from passing through it and ultimately reaching the detectors (the beam is said to be attenuated), denser areas seem darker**.** The image will also appear brighter in low-density areas since the beam will not be as attenuated there due to the detectors accumulating comparably more charge.

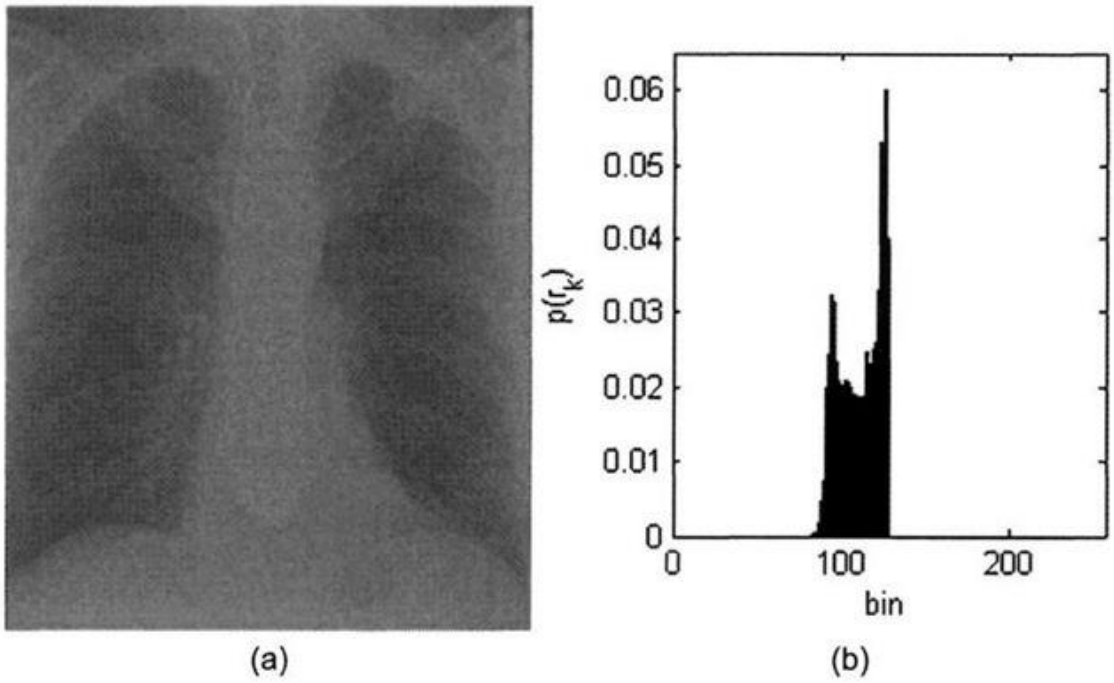

Fig 3.1: (a) Low contrast chest x-ray image, (b) Low contrast histogram [23]

The dense portions (bone) in Figures 3.1(a) and 3.2(a) seem white and the less dense areas (soft tissue and background) appear dark because it is normal practise to reverse the polarity of the acquired image when showing it by making the negative. The properties of the detectors and the amount of x-ray exposure the detectors absorb have a direct impact on the radiograph's overall quality.

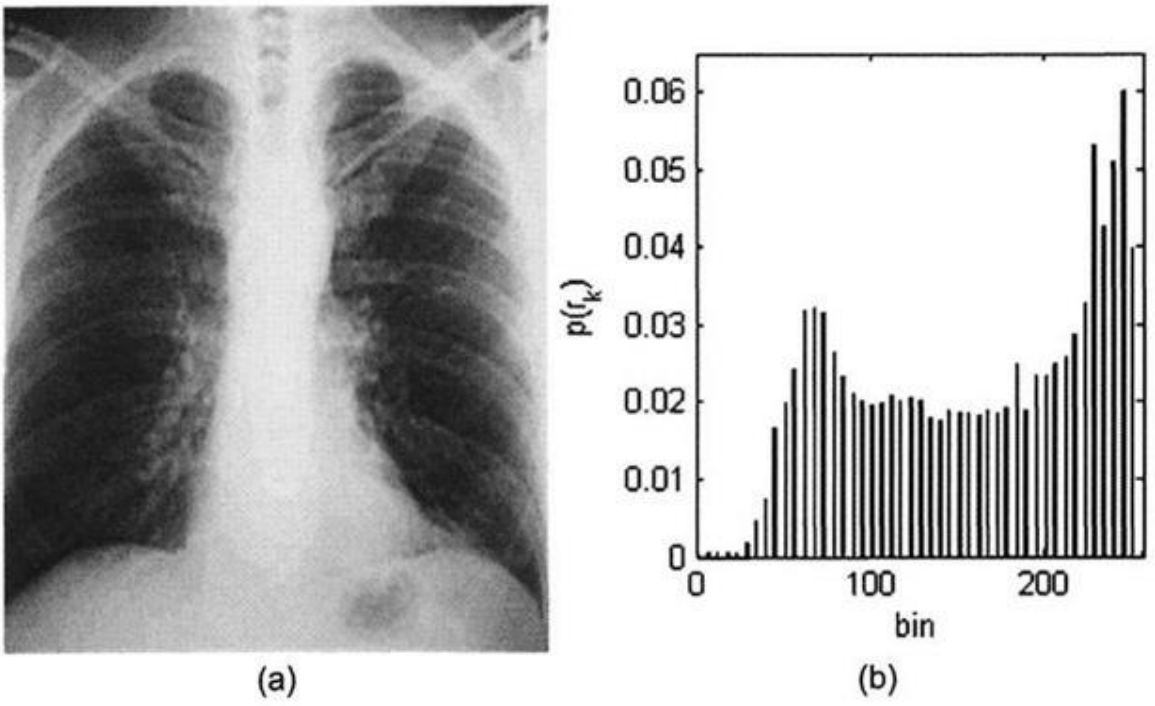

Fig 3.2: (a) Contrast-stretched chest x-ray image, (b) Modified histogram [24]

When there is insufficient light, the image seems low contrast and gloomy. A higher delta between pixel intensities corresponding to the bony parts and the background provides a better image with greater contrast (compare the quality of 3-1a with that of 3-2a). However, excessive illumination will saturate the image, causing the majority of pixel values to cluster in the higher part of the dynamic range and information loss as a result of clamping of grayscale intensities. Such a scenario is comparable to utilising an excessively high flash level when taking photographs, which results in a "washed out" image.

3.3 GRAYSCALE CONVERSION

The grayscale conversion is the following step that must be offered. The process of converting a picture from different colour spaces, such as RGB, CMYK, HSV, etc. to shades of grey is known as grayscale conversion. There are shades of black and white. In reality, a colour image 3D array is converted to a grayscale 2D array.

The formula takes into account the average of the red, green, and blue pixel values before adding the luminescence that each colour band contributes to create a respectable approximation of grey. A new matrix is created by weighting the sum of the red, green, and blue colour components to create a grayscale. For example the grayscale value at a location (x , y) can be given as :

$$\text{Grayscale value at } (x,y) = 0.299*R(i,j) + 0.587*G(i,j) + 0.114*B(i,j)$$

It means that in the particular image Red has contributed 29.9%, Green has contributed 58.7% and Blue has contributed nearly 11.4% . It is because after a lot of research it has been found that red color has more wavelength of all the three colors, and green is the color that has less wavelength than red color , besides giving a soothing effect to the eyes. It means, the contribution of red color has to decrease while the contribution of the green color has to increase. And the contribution by the blue colour has to be in between the red and green colour [25]. An illustration of RGB to grayscale converted image is shown Figure 3.3.

Fig. 3.3: image of a flower converted into grayscale [26]

3.3.1 Advantages of Grayscale Conversion:

Some of the advantages of using grayscale conversion are listed below [25]:

- For each colour component we need 8 beats so for RGB colour image that is 3 channels of colour we will need 8 * 3 equals 24 bits on the other hand if we use grayscale images then we will need only 8 bits to store an image pixel which reduces the memory size of a pixel by almost 2/3.
- It is also easier to apply image processing techniques on a single layered image than on a multi layered image.
- With grayscale images it is easier to detect edges and other important features.
- Processing a single layer image is much faster when it comes to processing images of mega pixels and that too running programs at a time parallel. While the same process will take 3 times mode if we use coloured image.

3.4 IMAGE BLURRING

A low pass filter is used to reduce the amount of noise as well as the amount of detail lost in an image, which is a phenomenon where the image loses details in the sharper parts. Another way to put it is that each pixel is mingled with its surrounding pixels, preventing the intensities of the pixels from remaining clearly distinct. Despite being undesirable in our images, this is incredibly helpful when performing image processing activities.

One of the most crucial image pre-processing procedures in the realm of image processing is smoothing and blurring. By smoothing, we may minimise undesirable noise and details ageing in an image. This does not mean that we will be removing the details of the features we are interested in but these are there are many edges in an image which are not required in our larger interest which can be eliminated by using this technique. There are 4 types of smoothing and blurring methods which are discussed below:

- simple average blurring
- Gaussian blurring
- median filtering
- bilateral filtering

  In this work of ours we have used the average blurring method using OpenCV.

3.4.1 Average blurring

This filter takes into account the pixels that surround a central pixel, calculates their average, and then substitutes the average value for the core pixel.

By averaging the area around a pixel, we smooth it out in this process and replace that pixel's value with that of its immediate neighbourhood. This lowers the level of details and noise. We must convolve the image with a P x Q normalised filter, where P and Q must both be odd numbers, in order to achieve average blur. For every pixel in the input image, the kernel in this case glides from top left to bottom right. The pixel at center of the kernel is set as the average of all the other pixels surrounding it. This is the reason an odd number is used to consider the matrix multiplication. The kernel matrix is given by the equation:

$$K = \frac{1}{kernel\ height * kernel\ width} \begin{bmatrix} 1 & 1 & 1 & 1 & 1 \\ 1 & 1 & 1 & 1 & 1 \\ 1 & 1 & 1 & 1 & 1 \\ 1 & 1 & 1 & 1 & 1 \\ 1 & 1 & 1 & 1 & 1 \end{bmatrix}$$

Let us consider an example to demonstrate this average blood using a 5 x 5 kernel which can be used to blur the central pixel with a 5 pixel radius.

$$K = \frac{1}{25} \begin{bmatrix} 1 & 1 & 1 & 1 & 1 \\ 1 & 1 & 1 & 1 & 1 \\ 1 & 1 & 1 & 1 & 1 \\ 1 & 1 & 1 & 1 & 1 \\ 1 & 1 & 1 & 1 & 1 \end{bmatrix}$$

In the matrix every element are given the same weights. Thus, an average value is considered for the 5 neighbouring pixel radius also with the increasing size of kernel the blooding of image will also increase accordingly.

Fig 3.4: An illustration showing the original and blurred image [27]

3.5 HOUGH CIRCLE TRANSFORM

The Hough transform is used to determine the lines in an image. The Hough transform is a key feature extraction technique used in digital image processing to locate circles in pictures with circular edges.

The following parametric equations can be used to define a circle with radius R and centres (a, b).

$$x = a + R\cos(\theta),$$
$$y = b + R\sin(\theta),$$

The points (x, y) trace the circumference of a circle as the angle swings through the whole 360 degree range. The search program's task is to identify parameter triplets (a, b, R) to characterise each circle if a picture has numerous points, some of which lie on circle perimeters. A direct use of the Hough algorithm would cost more in terms of computer memory and processing time due to the 3D nature of the parameter space [28].

3.5.1 Circle with Fixed Radius

The search can be condensed to 2D if the radius R of the circles in an image is known. Finding the coordinates of the centre (a, b) is our goal.

Let us consider the two equations given by:

$$x = a + R\cos(\theta)$$
$$y = b + R\sin(\theta)$$

The locus of the (a, b) points falls on a circle with radius R that is centred at (x, y). With the aid of a Hough accumulation array, the true centre point can be located. It will be shared by all parameter circles.

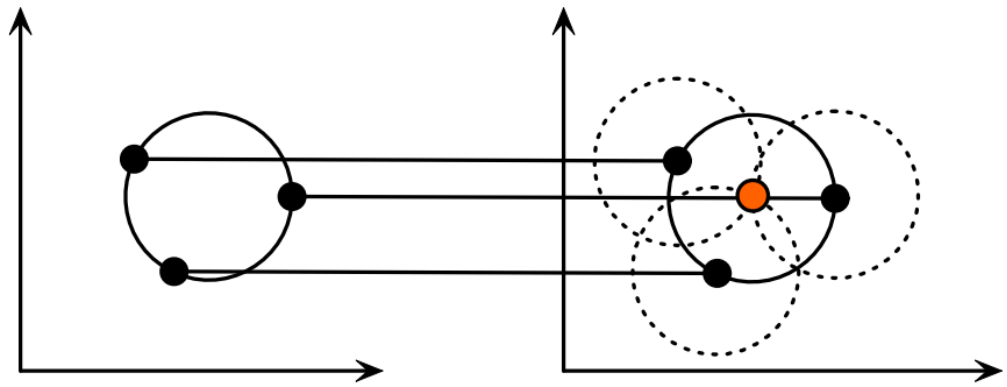

Fig 3.5: In parameter space, each point in geometric space (on the left) produces a circle (right). The circles in parameter space intersect at the (a, b) that is the center in geometric space [28]

3.5.2 Multiple Circles with known Radius

The same method can be used to locate several circles with the same radius. The parameter space depiction shows the center points as red cells. Circle overlap can result in the appearance of fictitious centres, as seen at the blue cell. Circles in the original image can be compared to remove extraneous ones.

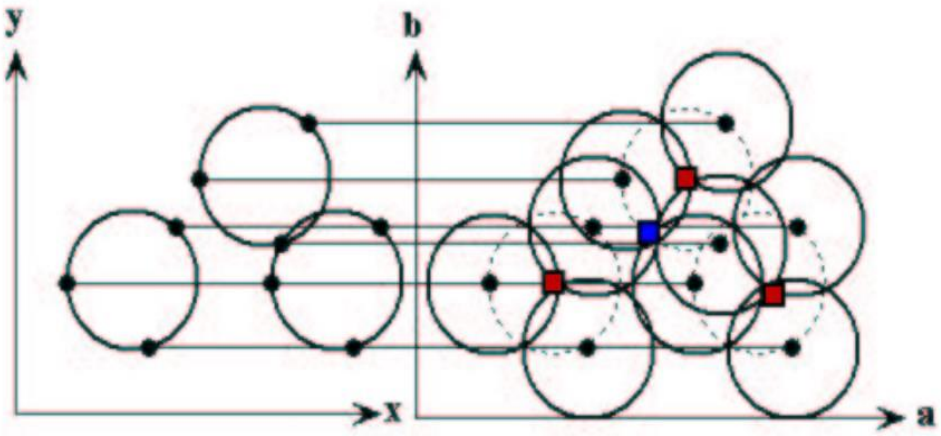

Fig 3.6: In parameter space, each point in geometric space (on the left) produces a circle (right). The circles in parameter space intersect at the (a, b) that is the center in geometric space [28]

3.5.3 Voting and the accumulation matrix

An accumulator matrix is used in practice to find the intersection point in the parameter space. We must divide the parameter space into "buckets" using a grid and then construct the matrix itself before we can establish an accumulator matrix. The number of "circles" in the parameter space that pass through the relevant grid cell in the parameter space is indicated by the element in the accumulator matrix. The "voting number" is another name for the number. At first, the matrix's elements are all zeros. The voting number of the grid cell that the circle passes through can then be increased for each "edge" point in the original space by formulating a circle in the parameter space. Voting is the action of doing this. Local maxima in the accumulator matrix can be located after voting. The locations of the local maxima line up with the original space's circle centres.

3.5.4 Finding circle parameter with unknown radius

The accumulator matrix would be 3D as well because the parameter space is 3D. We can iterate through potential radii, applying the prior method to each radii. Lastly, locate the 3D accumulator matrix's local maxima. In 3D space, the accumulation array should be A[x, y, c]. Each pixel, radius, and theta A[x, y, c] ± 1 should be eligible for voting.

The Algorithm:

Whenever A[a,b,r] = 0,

1. Apply the Gaussian Blurring filtering technique to the image, scale it to grayscale, then use the Canny operator to create the image's edges.
2. Cast as many votes as you can in the accumulator.
3. The circular Hough space is provided by the local maximum voted circles of Accumulator A. The Accumulator circle with the most votes wins the circle.

3.6 FLOWCHART OF THE PROCESS

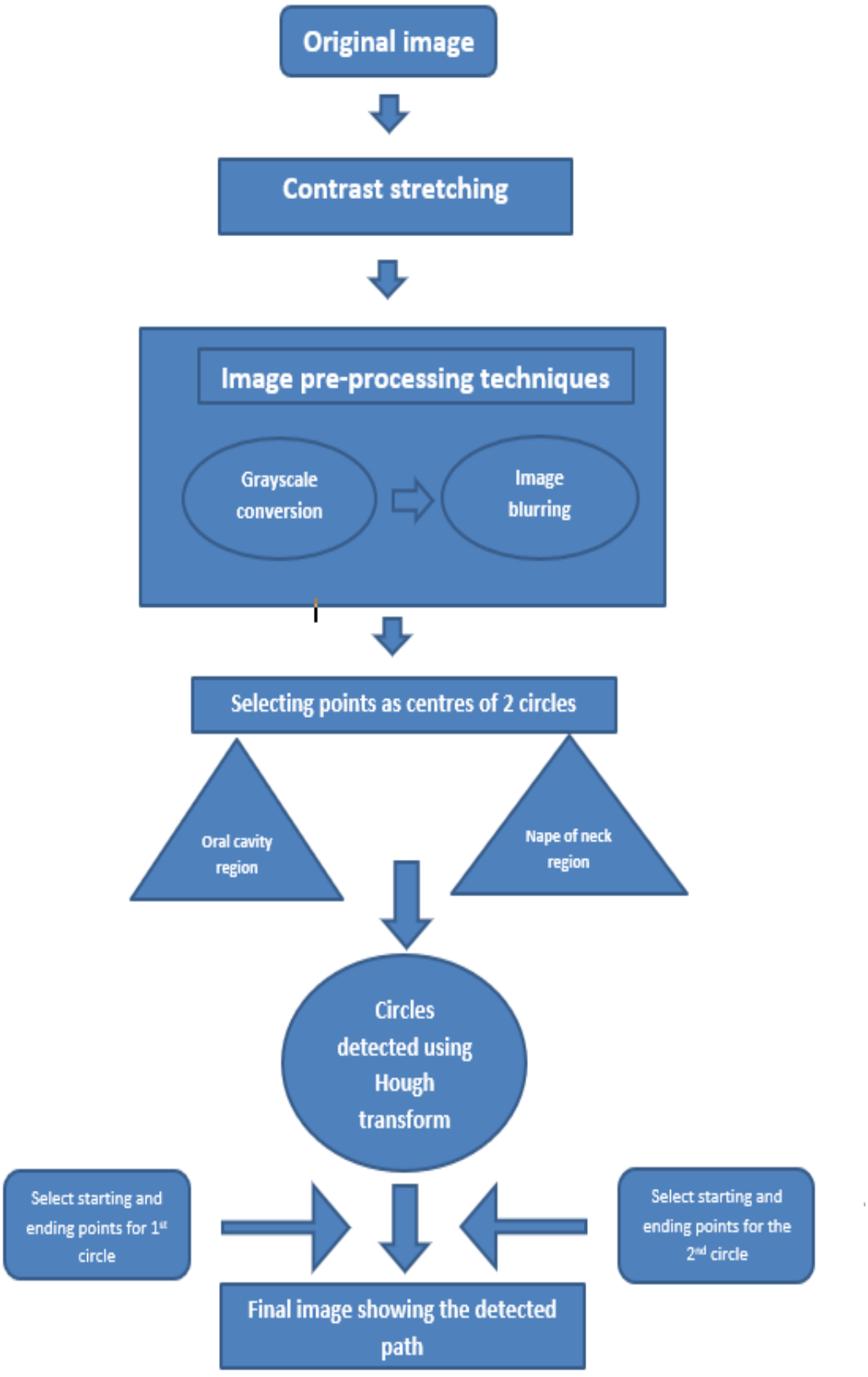

Fig 3.7: Flow chart of proposed algorithm

Chapter 4

Development of Graphical User Interface

4.1 GRAPHICAL USER INTERFACE

A Graphical User Interface, popularly known as GUI, is a special type of interface which allows the users to interact with electronic devices via visual indicator representations [29]. The GUI was first developed in the Xerox Palo Alto Research Laboratory in the late 1970s. It was commercially released in Apple's Macintosh and Microsoft's Windows operating systems, as a solution to the relatively ineffective usability issues of the early, text-based command-line interfaces for a typical user.

The GUI enables the user to intuitively operate computers and other electronic devices via the direct manipulation of graphical icons such as buttons, scroll bars, tabs, menus, cursors, windows. Especially the mouse pointing device has made graphical user interfaces the *de facto* standard of user-oriented design in software program-based applications. Moreover, the ability to interact with voice commands and touchscreens is now present in many contemporary graphical user interfaces.

A GUI utilizes pre-specified windows, icons, buttons, menus, etc. to execute operations which includes opening, modifying, deleting, moving files. A mouse is typically used to browse a GUI operating system. Keyboards are also used with specific shortcuts or the arrow keys. On a GUI system the mouse pointer is used to open the programme. To go to the directory where the programme is stored, list the files, and then launch the file using a command line interface, you must be familiar with the commands [30].

Here Python is used for the base programme of the GUI. The steps needed to follow in this regard are discussed next in details.

4.2 IMPORTING THE MODULES

4.2.1 Import cv2

The first step in the programming is to download the modules and libraries from which we would be using various functions packages to run the code. The most important among all is the open CV library. It is a sizable open-source library for image processing, machine learning, and computer vision, and it currently plays a significant part in real-time operations, which are crucial in modern systems [31]. Through the use of computer vision, one can comprehend the images and videos, how they are stored, and how to change and extract data from them. Using it, one can process photos and movies to look for things, people, or even human handwriting.

Applications of OpenCV:

OpenCV is used to solve many different problems; some of them are given below:

- Face recognition, automated inspection and monitoring, tally of people (such as foot movement in malls), the number of vehicles on highways, and the speeds of those vehicles are only a few examples.
- Interactive art exhibits
- Manufacturing process anomaly (defect) detection (the odd defective products)
- Street view picture stitching, video/image search and retrieval, navigation and control of robot and driverless cars, object recognition, medical image analysis, movies with 3D structure from motion, and TV channel ad recognition are just a few examples.

Functionality of OpenCV

Some of the functionalities of OpenCV are presented below:

- I/O, processing, and display of images and videos.
- Detecting objects or features
- Monocular or stereo computer vision based on geometry
- Computer-aided imaging (photo, video)
- Clustering and machine learning
- Acceleration using CUDA

4.2.2 Import NumPy

A general-purpose package for handling arrays is called NumPy [32]. It offers a multidimensional array object with outstanding speed as well as capabilities for interacting with these arrays. It is the cornerstone Python module for scientific computing. The programme is open-source. It has a number of characteristics, including the following crucial ones:

- A strong N-dimensional array object
- Complex (broadcasting) operations
- C/C++ and Fortran code integration tools; practical linear algebra, Fourier transform, and random number functions;

NumPy is a powerful multi-dimensional data container that has numerous applications outside of science. NumPy's ability to declare any data-types makes it possible for NumPy to quickly and easily interact with a wide range of databases.

4.2.3 Import Math

Mathematical calculations may occasionally be required when working on certain types of business or scientific tasks. Python includes the math module to cope with such calculations. Both simple operations like addition (+), subtraction (-), multiplication (*), and division (/) and advanced operations like trigonometric, logarithmic, and exponential functions are covered by the functions in the math module [33].

4.2.4 Import OS

Python's OS module offers tools for communicating with the operating system. OS is included in the basic utility modules for Python. This module offers a portable method of using functionality that is dependent on the operating system.

4.2.5 Import time

The Python time module, as the name suggests, enables working with time in Python. It enables features like obtaining the current time and stopping the programme from running, among others. Therefore, one must import this module before he/she begins.

There is no need to install the time module outside because it is included in the standard utility module for Python. Using the import command, one can import it quickly.

4.3 CREATING A CLICK_LIST VARIABLE

It is a tuple element of size N x 2 which is declared in the global scope so that it can be used globally as well as locally. By the term globally it means that this function can be recalled and put to use outside of the function as well. Whether used locally or globally it will use the same. The coordinates to be used will be saved in the variables.

Position refers to the index of the click list function. It is not used externally but it is used to initiate the tuple values in the click_list. For example, if the first value of the coordinate is (X_1, Y_1) then its position will be zero as the starting number in the index is zero in Python programming language.

4.4 APPLYING PRE-PROCESSING TECHNIQUES

First one needs to give an image as the input which will be read by the system. Next, some pre-processing techniques such as colour conversion, etc are applied. In colour conversion it is very important to change the image colour from its original form to grayscale. Then blurring phenomenon is applied to that grayscale image. This is done using suitable kernel size. The details of the average blur function and its technicalities have been discussed in Chapter 3.

4.5 CREATE A MOUSE CALLBACK FUNCTION

In this step, a mouse call-back function is developed which is executed when a mouse event takes place. Mouse event can be anything related to a mouse like left button down, left button up, left button double click, etc. It gives the coordinates X, Y for every mouse event. These events and locations will be used in the next stages of the program. Following a double click of the left button of the mouse X, Y values to a particular tuple variable will be stored.

In the next step an infinite loop is created where the system will wait for the user to provide input in the form of double click of the left button of the mouse using click list method.

When no input is given, that is, there is no data provided to the tuple of the click list, the system will show to choose the region in the oral cavity. Once a point is chosen in the oral cavity region it will confirm and proceed to the next step where it will ask the user to select the region near the nape of the neck. Again, when the two tuples (variables) are filled with the two data (coordinates)-(X_1, Y_1) and (X_2, Y_2) for the two required regions the system will show that all regions are selected and it will be detecting the possible circles.

The infinite loop will stop once both the required inputs are provided to the system.

4.6 APPLICATION OF THE HOUGH CIRCLE TRANSFORM WITH SUITABLE CONDITIONS

After selecting the regions, the system will be detecting the circles using the Hough circles. A detailed analysis of the Hough circle transform function has been discussed in Chapter 3.

Now the problem of using Hough circles detection method is that it will detect a large number of circles because this algorithm works to find circular edges in the images. So, it often happens that even a very small circular arc is detected and as a result one gets a large number of unwanted circles. To eradicate this problem, a condition has been included before the circles are detected. The condition is such that once the user have clicked on the oral cavity region and the neck region a loop will be run which will try to find a circle within a radius of 1 pixel from the input point. This loop will increase its radius count by one pixel up to 50 and go on trying to find a probable circle within that range.

Let us explain this mathematically.

Suppose the coordinates of the input clicked point be (x, y) and the center of the circle probably detected by using the Hough circle transform method be (a, b), then according to our condition given by distance formula it must satisfy the following criteria:

Distance < 50; or, $\sqrt{[(a - x)^2 + (y - b)^2]} < 50$

On the other hand, if the Hough circle is unable to find any circle within this range, then it will break out from the loop and show that no circle is detected.

4.7 METHODS APPLIED TO MARK THE START AND END POINTS ON THE CIRCLE

In the next step, the click list method is used again which has been declared globally earlier. This time the click list will be used to select the starting and ending points of both the circles because the objective is to get only the particular arc to detect the path and it is to be shown in the output. This small arc will be the path followed by the continuum robot during intubation. On this occasion the click list with will be used four times to store 4 coordinates in the tuple. Since the most important task is to find out the arc of that part of the circle which lies in the endotracheal region, so one needs to find out the angles of the two points in a particular circle with respect to the center of the circle in both the cases.

Let us illustrate this with the help of an example.

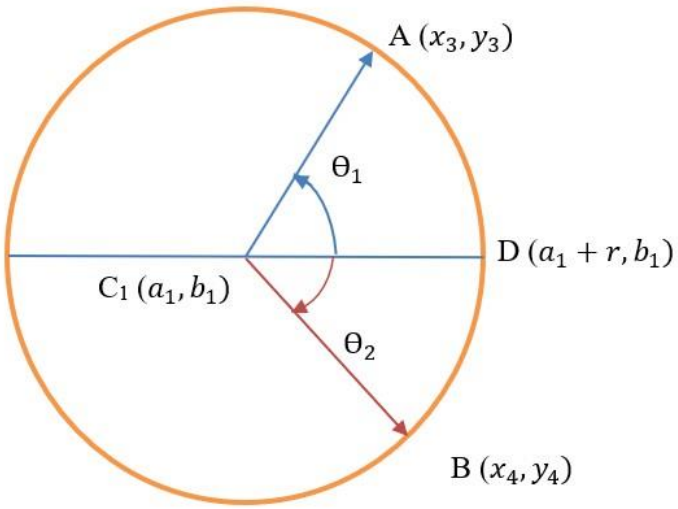

Fig 4.1: An illustration of points selected on a Hough circle with their angle orientation from the reference point D

Suppose, two points A (x_3, y_3) and B (x_4, y_4) have been selected.

The centre of the circle is given as C (a_1, b_1).

A straight line passing through the centre of the detected circle and parallel to the *x*-axis is considered as the reference angle which is 0 degree.

So let us consider the point D $(a_1 + r, b_1)$ as the reference point.

At first one needs to find the two angles Θ_1 and Θ_2.

Mathematically, to find the angle between two vectors, the dot product formula is used as shown below:

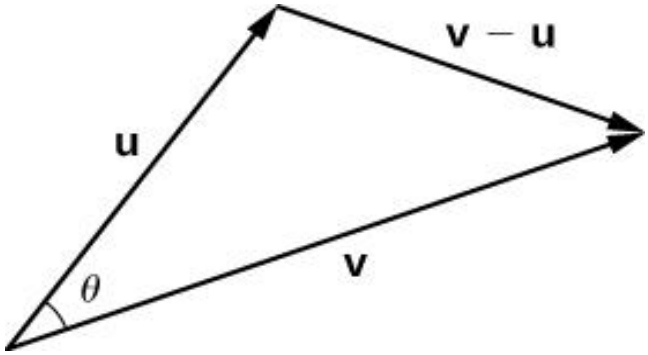

Fig 4.2: Angle formed by two vectors

It is well known that:

$$\vec{U}.\vec{V} = \text{U V cos}\,\Theta$$

$$\text{or,}\quad \cos\Theta = \frac{\vec{U}.\vec{V}}{UV}$$

$$\text{or,}\quad \Theta = \cos^{-1}\frac{\vec{U}.\vec{V}}{UV}$$

This formula can be used to find the positive and negative angles for both the circles.

Let us consider the first circle (in the region of oral cavity):

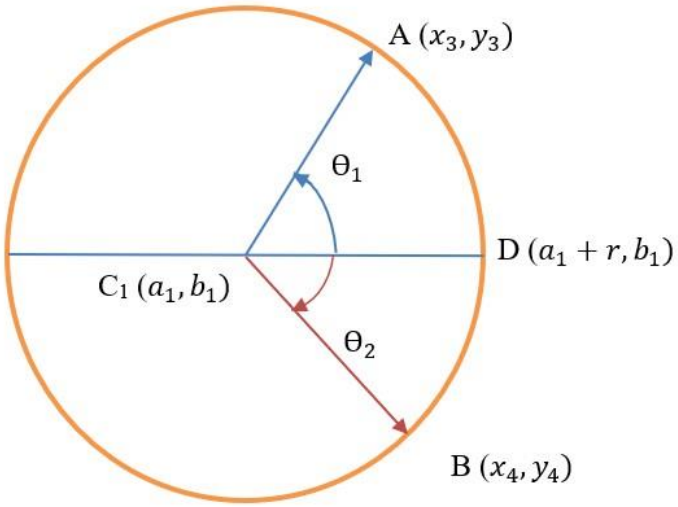

Fig. 4.3: Illustration of the two points (starting and ending) selected on the first detected circle

Let the starting point in case of the first circle be A (x_3, y_3) .

Let us consider $\Theta_1$as the starting angle, where $\Theta_1$is found out using the formula:

$$\Theta_1 = \cos^{-1} \frac{\vec{U}.\vec{V}}{U.V}$$

where U= $\vec{A} - \vec{C}$

and V= $\vec{D} - \vec{C}$

now let us set the condition as:

if $y_3 > b_1$, then Θ_1= positive

else if $y_3 < b_1$, then Θ_1= negative

otherwise Θ_1= 0

Similarly, let B be the ending point with ending angle Θ_2

where Θ_2 is found out using the formula:

$$\Theta_2 = \cos^{-1} \frac{U.V}{UV}$$

where U= $\vec{B} - \vec{C}$

and V= $\vec{D} - \vec{C}$

Now we set the condition as:

if $y_4 > b_1$, then Θ_2= positive

else if $y_4 < b_1$, then Θ_2= negative

otherwise Θ_2= 0

Similarly, let us consider the second circle (near the neck region):

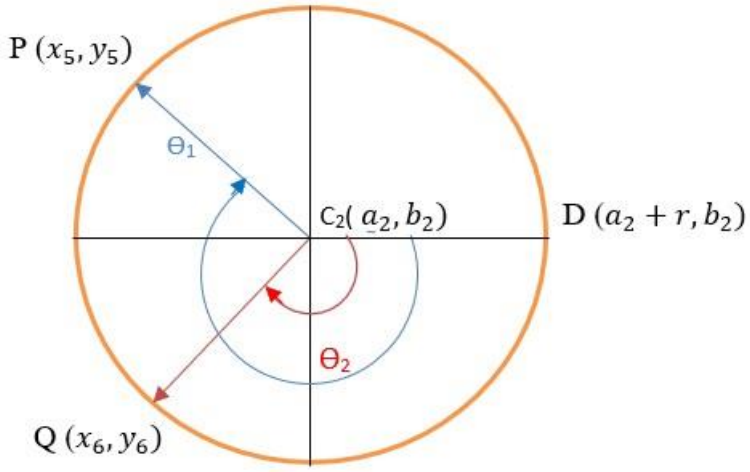

Fig. 4.4: Illustration of the selected points (starting and ending) on the second detected circle

Let us consider P to be the starting point.

In this case, let Θ_1 as the starting angle, where Θ_1 is found out using the formula:

$$\Theta_1 = \cos^{-1} \frac{\vec{U}.\vec{V}}{U.V}$$

where U= $\vec{P} - \vec{C}$

and V= $\vec{D} - \vec{C}$

Now, let us set the condition as:

if $y_5 > b_1$, then Θ_1= positive

else if $y_5 < b_1$, then Θ_1= negative

otherwise Θ_1= 0

Similarly, let Q be the ending point with ending angle Θ_2

where Θ_2 is found out using the formula:

$$\Theta_2 = \cos^{-1} \frac{\text{U.V}}{\text{UV}}$$

where U= $\vec{Q} - \vec{C}$

and V= $\vec{D} - \vec{C}$

Now, let us set the condition as:

if $y_6 > b_1$, then Θ_2= positive

else if $y_6 < b_1$, then Θ_2= negative

otherwise Θ_2= 0

4.8 APPLICATION OF THE ELLIPSE TRANSFORM FUNCTION TO GET THE FINAL ARC

In the final step, ellipse transform function will be used as it allows one to draw only a part of an ellipse or rather an arc of the curved path. This is simply because daily function in OpenCV takes into account the parameters such as starting and ending, which have already been determined in the previous stages and the values are stored as data.

The parameters to be taken into account while using the ellipse transform function are as follows:

centerCoordinates: These are the ellipse's centre coordinates. The coordinates are shown as pairs of two values, or tuples (X coordinate value, Y coordinate value).

axesLength: It contains a tuple of two variables with an elliptic curve's major and minor axes (major axis length, minor axis length).

Angle: The degree at which the ellipse is rotated.

startAngle: The elliptic arc's initial angle, measured in degrees.

endAngle: The elliptic arc's final angle, expressed in degrees.

Color: This is the hue of the border line of the proposed shape. We pass a tuple to BGR. As in (255, 0, 0) for the colour blue.

Chapter 5

Results and Discussions

Since we have considered four types of case studies for our thesis, so let us see the results obtained at various stages of each of these different cases.

5.1 Case 1: Normal endotracheal airway

In the first case, we will consider an image which shows the endotracheal cavity of a normal and healthy person.

The input CT image taken is shown in Fig 5.1:

Fig 5.1: The original image for normal airway

Apply contrast stretching

As the first step, we applied contrast stretching to the original image so that the region of our interest can be easily distinguished from the rest of the image. The contrast has to be set in such a way that even the minute details of our region of interest is restored while that of the unimportant regions are ruled out.

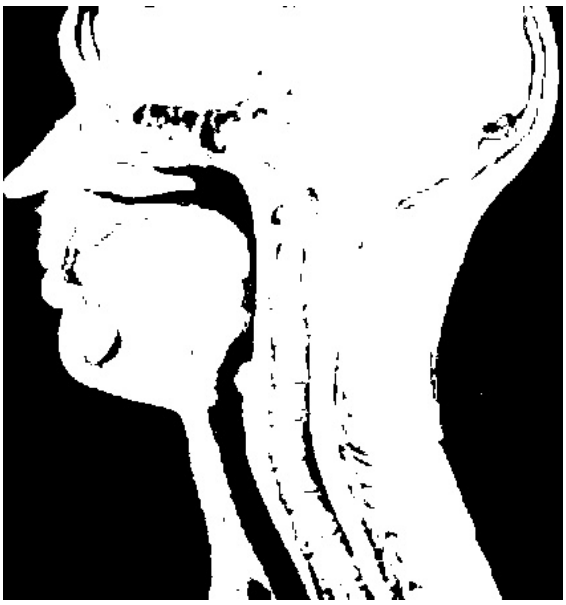

Fig 5.2: Image after contrast stretching for normal airway

Applying pre-processing techniques followed by hough circle transform

In this step some of the pre-processing techniques are applied such as grayscale conversion and blurring using a suitable kernel size. This is followed by detecting of circular edges using hough circle transform technique as discussed in Chapter 3.

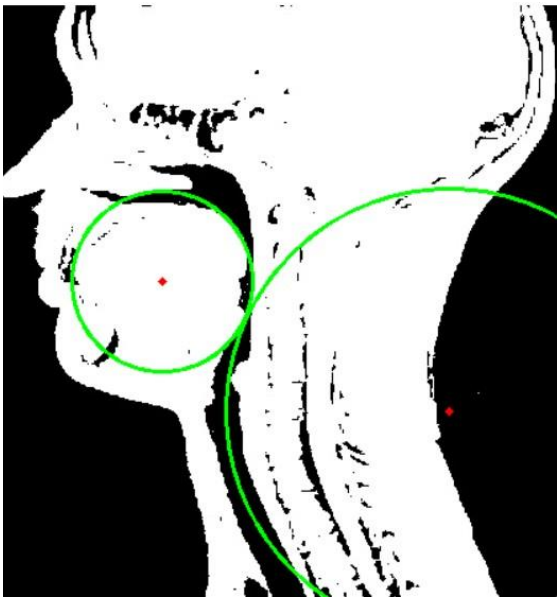

Fig. 5.3: Circles detected in the processed image for normal airway

Detection of the intubation path

In the final step, we need to select the starting and ending points of both the circles so that we get the final curved path in the endotracheal region.

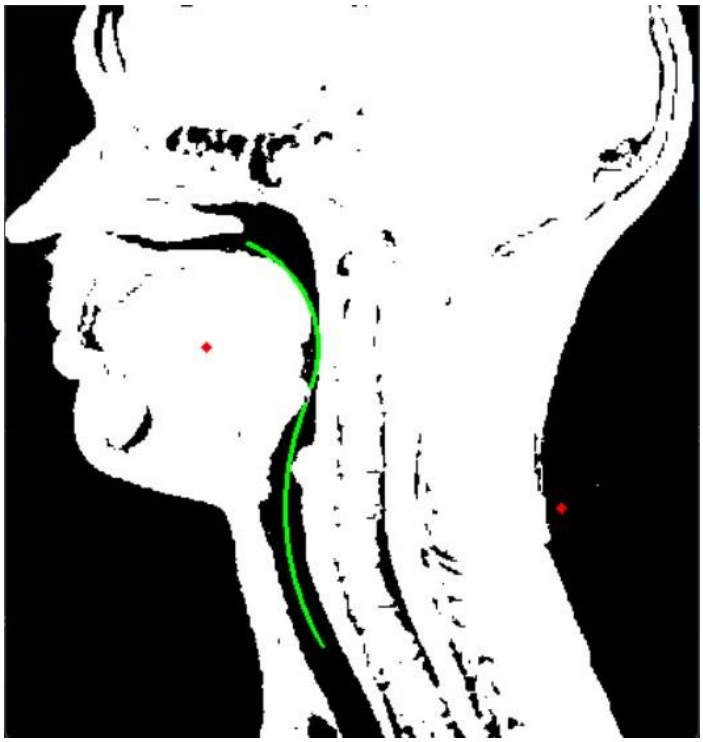

Fig 5.4: The final detected path for normal airway

The output parameters of the final image like the centres of the two circles, their radius, their starting and ending angles are shown in the tabulated form below:

Centre of the circle 1 : C_1 (x_1,y_1) =	(122,208)
Centre of the circle 2 : C_2 (x_2, y_2) =	(338,306)
Radius of the circle 1 : R_1	68
Radius of the circle 2 : R_2	168
Starting angle for circle C1 : SAc_1	-66.78°
Ending angle for circle C1 : EAc_1	17.36°
Starting angle for circle C2 : SAc_2	-159.65°
Ending angle for circle C2 : EAc_2	148.18°

5.2 Case 2: CT image of a patient with head injury

In the 2nd case study we consider an image of a patient with head injury. So there are some deformities in the nasopharyngeal region as seen from the CT scan.

So the original image is as shown below:

Fig 5.5: The original image for head injury

Apply contrast stretching

As the first step, we applied contrast stretching to the original image so that the region of our interest can be easily distinguished from the rest of the image. This image will serve as the input to our system for obtaining the desired results.

Fig 5.6: Image after contrast stretching for head injury

Applying pre-processing techniques followed by hough circle transform

In this step some of the pre-processing techniques are applied such as grayscale conversion and blurring using a suitable kernel size. This is followed by detecting of circular edges using hough circle transform technique.

Fig 5.7: Circles detected in the processed image for head injury

Detection of the intubation path

In the final step, we need to select the starting and ending points of both the circles so that we get the final curved path in the endotracheal region. The final image is shown in Fig.5.8.

Fig 5.8: The final detected path for head injury

The output parameters of the final image like the centres of the two circles, their radius, their starting and ending angles are shown in the tabulated form below:

Centre of the circle 1 : C_1 (x_1,y_1) =	(100,180)
Centre of the circle 2 : C_2 (x_2, y_2) =	(284,328)
Radius of the circle 1 : R_1	68
Radius of the circle 2 : R_2	165
Starting angle for circle C1 : SAc_1	-86.78°
Ending angle for circle C1 : EAc_1	57.36°
Starting angle for circle C2 : SAc_2	-149.65°
Ending angle for circle C2 : EAc_2	158.18°

5.3 Case 3: Patient with neck injury

In the 3rd case study we consider an image of a patient with neck injury. There are some deformities in the epiglottis region due to injury in the vertical column along the neck as seen from the CT scan.

So the original image is as shown in Fig. 5.9:

Fig 5.9: The original image for neck injury

Applying pre-processing techniques followed by hough circle transform

In this case , we will not be using the contrast stretching technique . instead we will directly be using image pre-processing techniques such as grayscale conversion and blurring using a suitable kernel size. This is followed by detecting of circular edges using hough circle transform technique. This method detects the circles in our region of interest.

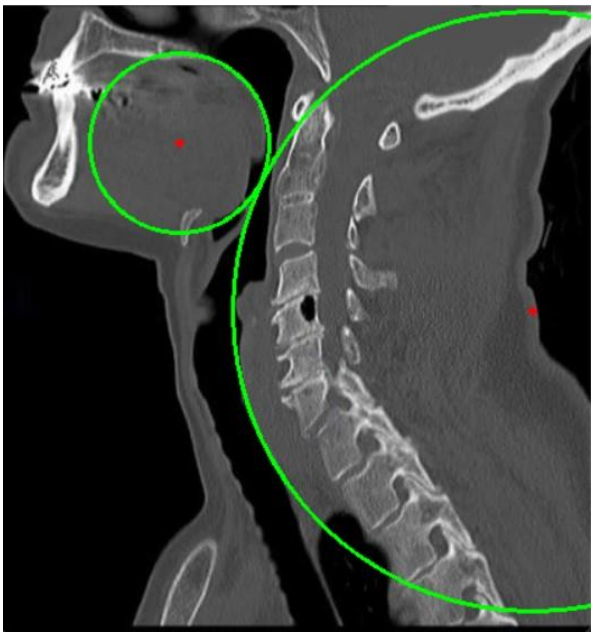

Fig. 5.10: Circles detected in the processed image for neck injury

Detection of the intubation path

In the final step, we need to select the starting and ending points of both the circles so that we get the final curved path in the endotracheal region.

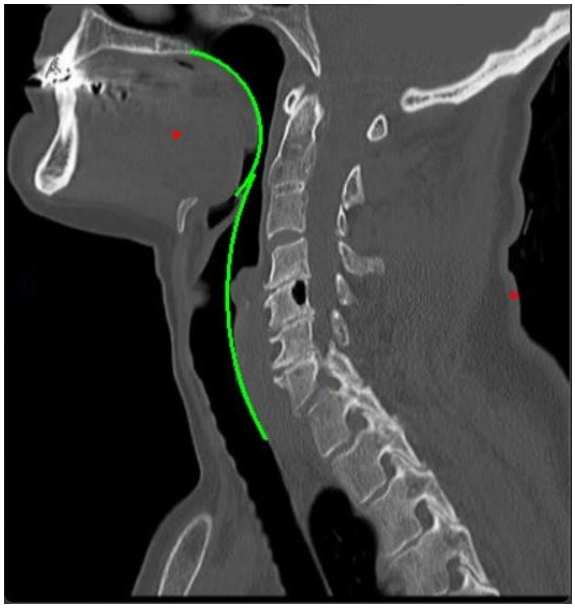

Fig 5.11: The final detected path for neck injury

The output parameters of the final image like the centres of the two circles, their radius, their starting and ending angles are shown in the tabulated form below:

Centre of the circle 1 : C_1 (x_1,y_1) =	(128,98)
Centre of the circle 2 : C_2 (x_2, y_2) =	(380,218)
Radius of the circle 1 : R_1	63
Radius of the circle 2 : R_2	184
Starting angle for circle C1 : SAc_1	-54.53°
Ending angle for circle C1 : EAc_1	22.39°
Starting angle for circle C2 : SAc_2	-157.65°
Ending angle for circle C2 : EAc_2	154.9°

5.4 Case 4: CT image of pediatric airway

In the 4th case study, we consider an image of the side view of the neck of a child. The airway of a child is quite different from a normal adult human in many respects. So, we have considered the paediatric airway as a case study to diversify our region of research.
In this case, the original image is shown below.

Fig 5.12: The original image for paediatric airway

Apply contrast stretching

As the first step, we applied contrast stretching to the original image so that the region of our interest can be easily distinguished from the rest of the image. The contrast has to be set in such a way that even the minute details of our region of interest is restored while that of the unimportant regions are ruled out.

This image will serve as the input to our system for obtaining the desired results.

Fig 5.13: Image after contrast stretching for paediatric airway

Applying pre-processing techniques followed by hough circle transform

In this step some of the pre-processing techniques are applied such as grayscale conversion and blurring using a suitable kernel size. This is followed by detecting of circular edges using hough circle transform technique . this method detects the circles in our region of interest as shown in Fig 5.14.

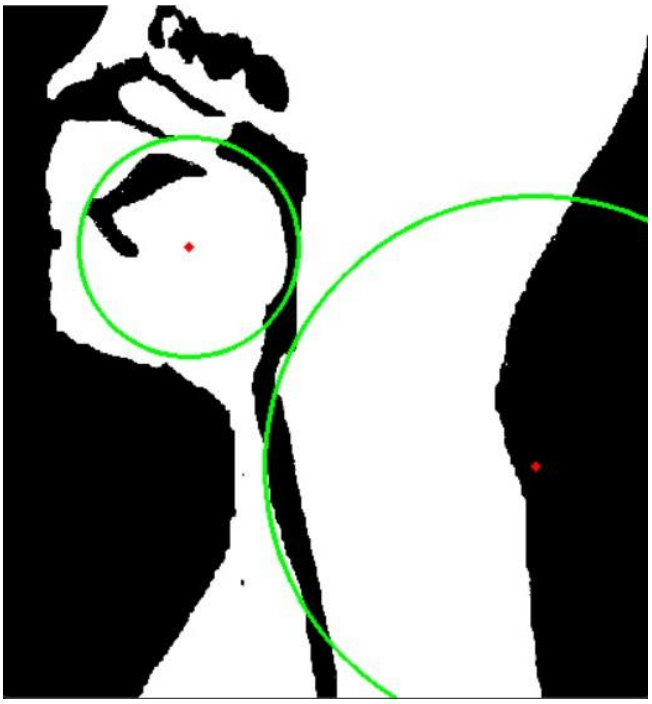

Fig. 5.14: Circles detected in the processed image for paediatric airway

Detection of the intubation path

In the final step, we need to select the starting and ending points of both the circles so that we get the final curved path in the endotracheal region. The final image is shown in Fig 5.15.

Fig 5.15: The final detected path for paediatric airway

The output parameters of the final image like the centres of the two circles, their radius, their starting and ending angles are shown in the tabulated form below:

Centre of the circle 1 : C_1 (x_1,y_1) =	(122,156)
Centre of the circle 2 : C_2 (x_2, y_2) =	(346,298)
Radius of the circle 1 : R_1	71
Radius of the circle 2 : R_2	175
Starting angle for circle C1 : SAc_1	-53.37°
Ending angle for circle C1 : EAc_1	30.8°
Starting angle for circle C2 : SAc_2	-150.34°
Ending angle for circle C2 : EAc_2	147.4°

Chapter 6

Applications, Conclusion and Future work

6.1 APPLICATION I: FEATURE EXTRACTION OF THE SOFT TRACHEAL TUBE FOR PASSIVE INTUBATION

In this thesis, two main applications of the developed endotracheal path detection algorithm are proposed. The first application is related to passive intubation where a soft/flexible tube is inserted in the trachea and the movement of the tube is driven by tendons that are operated using precise robotic system placed outside the patient's body. Such passive soft/ flexible tubes are [51], [52] made of bio compatible materials and are mostly designated for single use only.

From the design and modelling point of view, these tubes are considered as soft multi-body systems. Several works are found in literature, where the geometric and unified model of the tube is derived based on discrete Cosserat approach and backward recursion method of the soft-body dynamics [51], [52], [53]. The material used for constructing the tube is generally a material with low Young's moduli. Therefore, the elasticity of the material and the type of actuation used will introduced complexity to the unified model.

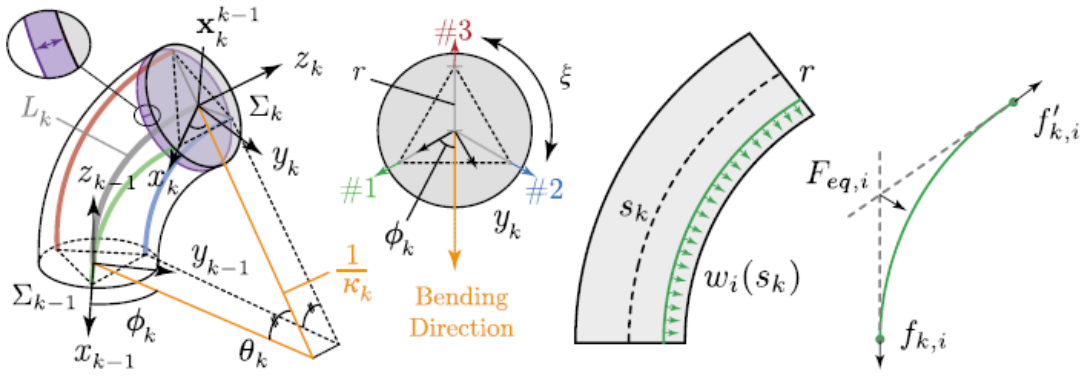

Fig 6.1: Sketch of tendon-driven soft/flexible tube (left), Simplified 2-DOF representation (right)

The most common approach used for modelling such a soft tendon driven system is geometry-based piecewise constant curvature approach. Assuming the tube backbone length to be constant, piecewise constant curvature approach would simplify the soft/flexible tube segment into a 2-DOF module as shown in Fig. 6.1. Now, for a multi-segment soft tube, with n segments, the k-th soft segment ($k \leq n$) can be geometrically parameterized in the configuration space by

$$\boldsymbol{\psi}_k = [\vartheta_k, \varphi_k, \kappa_k]$$

where, $\vartheta_k \in [0, \vartheta_{max}]$ is the angle of bending,

$\varphi_k \in [-\pi, \pi)$ is the angle of bending direction,

κ_k is the bending curvature

L_k is the initial undeformed length of the segment

and $\kappa_k = \vartheta_k / L_k$.

Thus, the position of the k-th segment with respect to its base frame $\sum_{k-1}$ can be expressed by

$$x_k^{k-1} = \frac{1}{K_k}\begin{bmatrix}\cos\varphi_k(1-\cos\theta_k)\\ \sin\varphi_k(1-\cos\theta_k)\\ \sin\theta_k\end{bmatrix}$$

From the results obtained in the previous chapter of the thesis, the segment of endotracheal path, that needs to be imitated by the soft/ flexible tube, can be selected. A given segment of the endotracheal path can be represented as a concatenation of standard conic section arcs and, therefore, θ_k and φ_k can be obtained from the selection. Next, the features of the soft/flexible tube like length of the tube, bending curvature, radius are calculated using the following equations. The bending curvature is obtained following the relation:

$$K_k = \frac{\theta_k}{L_k}$$

From these values next the actuations provided by the tendons of the soft/flexible tube can be calculated. Let, $q_{k,i} \subseteq \boldsymbol{q}_k$ be the actuation-by-length of the i-th cable of k-th segment, given by the subtraction of the in-body cable length $L_{k,i}$ and the length of the neutral line L_k and r be the (constant) symmetric distance between the centre of the cross-section and the cable channel. Then the actuation required can be calculated as

$$q_{k,i} = L_{k,i} - L_k = -\theta_k r\cos(\varphi_k + (i-1)\varepsilon)$$

Where, $i \in \{1, 2, 3\}$ and $\varepsilon = 2\pi/3$.

6.2 APPLICATION II: ESTIMATION OF SAFE ENTRANCE MECHANISM FOR A CONTINUUM ROBOT TO EXECUTE ENDOTRACHEAL INTUBATION

The second application of the developed endotracheal path detection algorithm is to estimate the safe entrance mechanism for a continuum robot to execute endotracheal intubation. In the last decade, robots have become an integral part of operating rooms around the world and have assured the possibility of introducing or improving many new minimally invasive surgical procedures. It is an accepted reality that minimally invasive surgery is preferable because it can reduce patient discomfort, operating costs, and hospital time. The use of robotic technology in surgery brings precision, intuitive ergonomic interfaces, and the ability to access surgical sites remotely with miniaturized instrumentation. Thus, robotics has the potential to further advance the benefits of minimally invasive surgery and make new procedures possible.

Therefore, it is evident that the trend is toward minimally invasive surgery and robotics has enabled enhanced performance in minimally invasive abdominal surgery, adaption to areas requiring more delicate, circuitous, access is challenging. Thus, it would be highly beneficial to have manipulators which are scalable to a small size, flexible yet strong, and which can reach difficult-to-access surgical sites via nonlinear pathways and complete the surgical task with dexterity. There is a promising category of robots that are capable of providing these features: continuum robots. Several works are done [38], [39], [40] on development of continuum robots, some of the designs are provided in Fig 6.2.

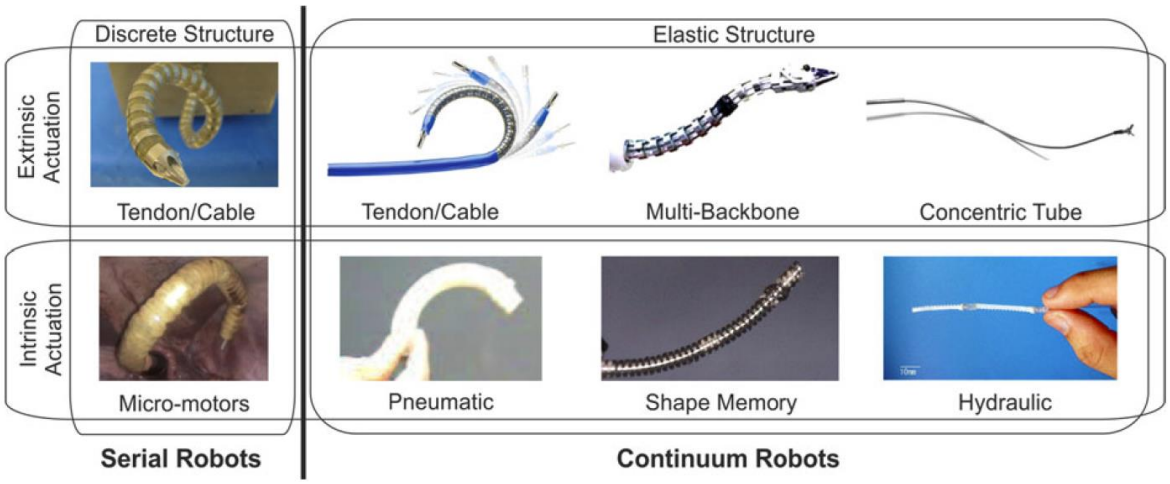

Fig 6.2: Different continuum robot designs

A simple but broad-spectrum definition of continuum robot would be:

Definition: A continuum robot is an actuatable structure whose constitutive material forms curves with continuous tangent vectors.

Continuum robots have a fundamental difference with the structure of the conventional manipulators composed of discrete rigid links connected by joints. When a robot has more degrees of freedoms (DOFs) than are necessary to execute a task, (e.g., a 7-DOF arm with 6-DOF task space), it is said to be redundant or in extreme cases, hyper-redundant [41]. In the limit as the number of joints approaches infinity (and the link lengths approach zero), the robot approaches what is known as a continuum robot [42]. The shape and structure of a continuum robot are defined by an infinite-DOF elastic member. Generally, continuum robots can be constructed at smaller scales than those robots with discrete links due to the simplicity of their structures (see Fig. 6.2).

Kinematic Frameworks: The most familiar kinematic framework for roboticists is the discrete approach employed in conventional rigid-link manipulator models. In this approach, a series of rigid links connected by conventional revolute, universal, or spherical joints is described using a series of homogeneous transformations generated from standard Denavit–Hartenberg (D–H) parameter tables. Of course, these models are entirely appropriate in the case of the discrete structure manipulators, but discrete models can also provide good approximate representations of continuous elastic structures. Medical continuum robots that have used a discrete rigid link kinematic framework include [43] and [44]. In contrast with rigid-link models, constant-curvature kinematic frameworks represent continuum robot geometry with a finite number of mutually tangent curved segments each having a constant curvature along its length. Note that “constant” here refers to invariance with respect to arc length, not time.

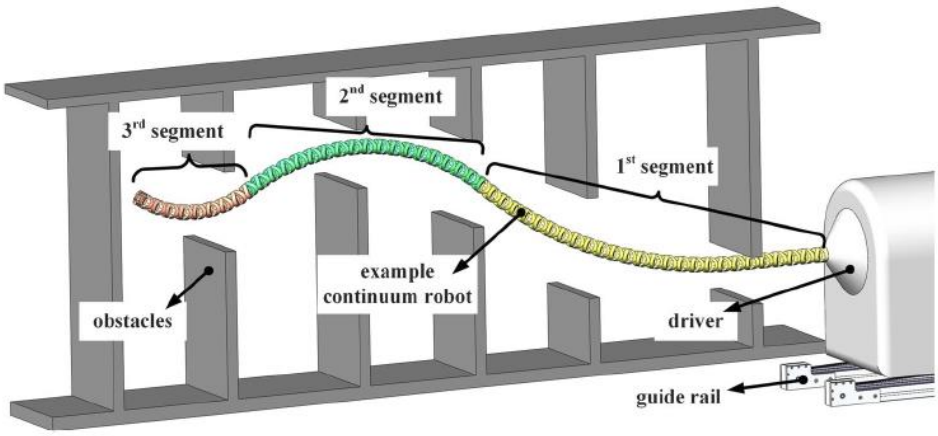

Fig 6.3: Application of continuum bending in a narrow space

In this framework, the curvature, length, and angle (known as the “arc parameters”) of each segment form a set of configuration coordinates that completely describes the shape of the robot, i.e., the position and orientation at any point on the robot can be written as a function of the arc parameters and the arc length along the backbone to that point. Similar to D–H parameters, each arc parameter could be a constant or vary with actuation, depending on the robot design. Usually, a single constant-curvature segment is employed for each actuatable section of the robot. However, some work has also employed constant-curvature segments as the basis for a discretization scheme within an actuated segment [45], [46]. This approach is similar to the rigid-link framework, but it provides a more visually realistic geometric approximation.

Constant curvature is perhaps the most well-known and widely used kinematic framework for continuum robots, and the homogeneous transformation along a constant-curvature robot backbone has been derived from a variety of perspectives, such as D–H parameters [47], [48], Frenet–Serret frames [48], integral representation [49], and exponential coordinates [50], [51]. Webster and Jones have devoted a large portion of their review paper [52] to showing equivalency between these formulations, and we refer the interested reader to their paper for the details of the constant-curvature transformation matrix. The proposed identified endotracheal path is a concatenation of constant curvature segments. These segments can be used as the input to the transformation matrix to obtain the actuation commands.

6.3 CONCLUSION

This thesis, identifies the problems related to video laryngoscopy using top view images of trachea and proposes a detection algorithm to estimate the orientation of the endotracheal path using image processing techniques. The techniques used comprises of several steps, which include image enhancement, contrast stretching, grayscale conversion, image blurring and Hough circle transform.

For developing the algorithm CT scan images of side view of the neck are used. The detection of the intubation path with such an image will help in finding the orientation of the path and in turn help in the insertion of robot into the trachea.

A Graphical User Interface is developed in this regard and the design steps of the same are also presented. The application of the Hough transforms with suitable conditions for finding

the conic sections such as circles and ellipse are discussed. Methods applied to mark the start and end points of the circular segments are discussed in details.

To address a broader spectrum of clinical difficulties the results obtained from the algorithm developed are presented and the interpretations of the results are discussed for four different cases (i) normal endotracheal airway, (ii) patient with head injury, (iii) patient with neck injury, (iv) pediatric airway.

Finally, this thesis points out two major application of the developed algorithm for detection of endotracheal path. This detection algorithm may be employed to calculate approximate curvature, diameter and length of the soft/flexible tracheal tube used in passive intubation. Another application of the algorithm could be estimating a safe entrance mechanism for a continuum robot to execute active robotic endotracheal intubation.

6.4 FUTURE WORK

The algorithm developed is based on CT scan images of side view of the neck, this can be extended algorithms based on images that are captured using non-ionised rays such as MRI images.

The present algorithm employs edge detection technique based on Hough Transform. Here, circular transform is considered in majority of the cases keeping in mind the constant-curvature property of soft tube or continuum robot. One may explore the possibility of other conic section arcs like ellipse, parabola and hyperbola detection as a topic of future study.

Moreover, with availability of proper dataset regarding side view images of neck region, Machine Learning techniques can be incorporated to automate the detection of endotracheal path with greater accuracy.

Finally, based on the endotracheal path as detected by the proposed algorithm the trajectory and motion planning of a soft robotic tube or a continuum robot can be instrumented.

References

[1] T. Ezri , S. Evron, H. Hadad and Y. Roth, " Tracheostomy and endotracheal intubation: a short story," Department of Anesthesia, The Edith Wolfson Medical Center, vol. 144, no. 12 , 2005.

[2] E. B. Thomas and S. Moss, "Tracheal intubation," Anaesthesia Intensive Care Med., vol. 15, no. 1, pp. 5–7, Jan. 2014.

[3] Reed, M. J., Dunn, M. J. G., & McKeown, D. W."Can an airway assessment score predict difficulty at intubation in the emergency department?. Emergency medicine journal", 22(2), pp. 99-102,2005.

[4] Shaik Naseera, G.K. Rajini, B. Venkateswarlu, Jasmin Pemeena Priyadarisini M, "A review on application of image processing in medical field". Research Journal of Pharmacy and Technology, pp. 3456-3460, October 2017.

[5] Apfelbaum, J. L., Hagberg, C. A., Caplan, R. A., Blitt, C. D., Connis, R. T., and Ovassapian, A., "Practice guidelines for management of the difficult airway," Anesthesiology, vol. 118, no. 2, pp. 251–270, Feb. 2013.

[6] P. E. Pepe, L. P. Roppolo, and R. L. Fowler, "Prehospital endotracheal intubation: Elemental or detrimental?" Crit. Care, vol. 19, no. 1, pp. 121, Mar. 2015.

[7] D. B. Glick, R. M. Cooper, and A. Ovassapian, " The Difficult Airway: An Atlas of Tools and Techniques for Clinical Management," New York, USA: Springer, 2013.

[8] K. McCluskey and M. Stephens, "Alternative techniques for tracheal intubation," Anaesthesia Intensive Care Med., vol. 18, no. 4, pp. 163–167, Apr. 2017.

[9] Shippey, B., Ray, D., & McKeown, D. , "Use of the McGrath R _ video laryngoscope in the management of difficult and failed tracheal intubation," British journal of anaesthesia, 100(1),pp. 116-119, 2008.

[10] Huitink, J. M., Koopman, E. M., Bouwman, R. A., Craenen, A., Verwoert, M., Krage, R., & Schauer, A. , "Tracheal intubation with a camera embedded in the tube tip (VivasightTM)," Anaesthesia, 68(1), 74-78, 2013.

[11] Anesthesiologist performs tracheal intubation for patient," Time. Available: https://www.dreamstime.com/anesthesiologist-performs-tracheal-intubation-patient-operation-room-image165650093.

[12] "Photo about This is the picture of ventilator and instruments for intubation, anesthesia, emergency care . Image of intubation, maintain, mobile - 5275280," Time. Available: https://www.dreamstime.com/stock-photo-anaestesia-operation-set-image5275280#.

[13] Cormack, R. S., & Lehane, J. (1984). Difficult tracheal intubation in obstetrics. Anaesthesia, 39(11), 1105-1111.

[14] "The endotracheal tube in detail," Derangedphysiology.com. [Online]. Available: https://derangedphysiology.com/main/required-reading/equipment-and-procedures/Chapter%202812/endotracheal-tube-detail.

[15] J. M. Huitink, D. R. Buitelaar, and P. F. E. Schutte, "Awake fibrecapnic intubation: A novel technique for intubation in head and neck cancer patients with a difficult airway," Anaesthesia, vol. 61, no. 5, pp. 449–452, May 2006.

[16] J. E. Archer and A. Gardner, "A case of missed unstable cervical injury during the COVID-19 pandemic," J. Surg. Case Rep., vol. 2020, no. 9, p. rjaa293, 2020. Cooper, R. M., Pacey, J. A., Bishop, M. J., & McCluskey, S. A. (2005). Early clinical experience with a new video laryngoscope (GlideScope R _) in 728 patients. Canadian Journal of Anesthesia, 52(2), 191.

[17] A. Y. Tumu, T. Chandra, M. Maheshwari, T. G. Kelly, and H. D. Segall, "Imaging of pediatric aerodigestive tract disorders," Neurographics, vol. 4, no. 1, pp.33-42, 2014.

[18] Tariq M. Wani et al., "age based analysis of paediatric upper airway dimensions using CT imaging", Pediatric Pulmonology, pp.:267–271, 2016.

[19] R. J. Gaspari, A. J. Singer, and H. C. Thode, "Magnetically guided orotracheal intubation," Acad. Emerg. Med., vol. 8, no. 3, pp. 285–287, Mar. 2001.

[20] S. Bilge, O. Tezel, Y. A. Acar, G. Aydin, A. Aydin, and G. Ozkan, "Endotracheal intubation by paramedics using neodymium magnet and modified stylet in simulated difficult airway: A prospective, randomized, crossover manikin study," Emerg. Med. Int., vol. 2019, p. 5804260, 2019.

[21] T. Hemmerling, R. Taddei, M. Wehbe, C. Zaouter, S. Cyr, and J. Morse, "First robotic tracheal intubations in humans using the Kepler intubation system," Brit. J. Anaesthesia, vol. 108, no. 6, pp. 1011–1016, Jun. 2012.

[22] Q. Boehler et al., "REALITI: A Robotic Endoscope Automated via Laryngeal Imaging for Tracheal Intubation," in IEEE Transactions on Medical Robotics and Bionics, vol. 2, no. 2, pp. 157-164, May 2020, doi: 10.1109/TMRB.2020.2969291.

[23] What-when-how.com. [Online]. Available: https://what-when-how.com/wp-content/uploads/2011/09/tmp648_thumb.jpg.

[24] "Contrast stretched image with histogram", https://what-when-how.com/wp-content/uploads/2011/09/tmp649_thumb.jpg.

[25] Hrithik Salgaokar,"grayscale conversion", Available: https://www.geeksforgeeks.org/matlab-rgb-image-to-grayscale-image-conversion/,

[26] Github.io. [Online]. Available: https://dev-akash.github.io/images/grayscale-conversion.PNG-grayscale.

[27] Zhang Chinen, "Image blurring", Available: https://codeloop.org/wpcontent/uploads/2020/08/avarage_burring_opencv.jpg - blurr..

[28] Harvey Rhody, "lecture on hough circle transform", Chester F. Carlson Center for Imaging Science Rochester Institute of Technology , October 11, 2005.

[29] "Graphical User Interface," Heavy.ai. Available:https://www.heavy.ai/technical-gloassary/graphical-user-interface.

[30] A. Kay and D. Engelbart, "What is a GUI (Graphical User Interface)?," Computerhope.com. Available: https://www.computerhope.com/jargon/g/gui.htm.

[31] "How to install OpenCV for python on windows?," GeeksforGeeks, 21-Jan-2020. Available:https://www.geeksforgeeks.org/how-to-install-opencv-for-python-in-windows/.

[32] "NumPy in python," GeeksforGeeks, 31-Jan-2017. [Online]. Available: https://www.geeksforgeeks.org/numpy-in-python-set-1-introduction/.

[33] "Python math module," *GeeksforGeeks*, 17-Jun-2021. [Online]. Available: https://www.geeksforgeeks.org/python-math-module/.

[34] S. W. Jensen, C. C. Johnson, A. M. Lindberg and M. D. Killpack, "Tractable and Intuitive Dynamic Model for Soft Robots via the Recursive Newton-Euler Algorithm," *2022 IEEE 5th International Conference on Soft Robotics (RoboSoft)*, 2022, pp. 416-422.

[35] J. Lai, B. Lu, Q. Zhao and H. K. Chu, "Constrained Motion Planning of a Cable-Driven Soft Robot With Compressible Curvature Modeling," in *IEEE Robotics and Automation Letters*, vol. 7, no. 2, pp. 4813-4820, April 2022.

[36] F. Renda and L. Seneviratne, "A Geometric and Unified Approach for Modeling Soft-Rigid Multi-Body Systems with Lumped and Distributed Degrees of Freedom," *2018*

IEEE International Conference on Robotics and Automation (ICRA), 2018, pp. 1567-1574.

[37] B. Deutschmann, J. Reinecke and A. Dietrich, "Open Source Tendon-driven Continuum Mechanism: A Platform for Research in Soft Robotics," *2022 IEEE 5th International Conference on Soft Robotics (RoboSoft)*, 2022, pp. 54-61.

[38] M. A. Mandolino, Y. Goergen, P. Motzki and G. Rizzello, "Design and Characterization of a Fully Integrated Continuum Robot Actuated by Shape Memory Alloy Wires," *2022 IEEE 17th International Conference on Advanced Motion Control (AMC)*, 2022, pp. 6-11.

[39] J. Burgner-Kahrs, D. C. Rucker and H. Choset, "Continuum Robots for Medical Applications: A Survey," in *IEEE Transactions on Robotics*, vol. 31, no. 6, pp. 1261-1280, Dec. 2015.

[40] Wu, H., Yu, J., Pan, J. *et al.*, "CRRIK: A Fast Heuristic Algorithm for the Inverse Kinematics of Continuum Robot", *J Intell Robot Syst*, vol. 105, no. 55 (2022).

[41] K. Xu and N. Simaan, "An Investigation of the Intrinsic Force Sensing Capabilities of Continuum Robots," in *IEEE Transactions on Robotics*, vol. 24, no. 3, pp. 576-587, June 2008.

[42] F. Zaccaria, E. Idá, S. Briot and M. Carricato, "Workspace Computation of Planar Continuum Parallel Robots," in *IEEE Robotics and Automation Letters*, vol. 7, no. 2, pp. 2700-2707, April 2022.

[43] M. D. M. Kutzer, S. M. Segreti, C. Y. Brown, M. Armand, R. H. Taylor, and S. C. Mears, "Design of a new cable-driven manipulator with a large open lumen: Preliminary applications in the minimally-invasive removal of osteolysis," in *Proc. IEEE Int. Conf. Robot. Autom.*, 2011, pp. 2913–2920.

[44] Y. Ganji and F. Janabi-Sharifi, "Catheter kinematics for intracardiac navigation," *IEEE Trans. Biomed. Eng.*, vol. 56, no. 3, pp. 621–32, Mar. 2009.

[45] W. S. Rone and P. Ben-Tzvi, "Mechanics modeling of multisegment rod-driven continuum robots," *J. Mech. Robot.*, vol. 6, no. 4, p.p. 041006, 2014.

[46] M. Dehghani and S. A. A. Moosavian, "Modeling of continuum robots with twisted tendon actuation systems," in *Proc. RSI/ISM Int. Conf. Robot. Mechatron.*, 2013, pp. 14–19.

[47] B. A. Jones and I. D. Walker, "Kinematics for multi-section continuum robots," *IEEE Trans. Robot.*, vol. 22, no. 1, pp. 43–55, Feb. 2006.

[48] M. W. Hannan and I. D. Walker, “Kinematics and the implementation of an elephant’s trunk manipulator and other continuum style robots,” *J. Robot. Syst.*, vol. 20, no. 2, pp. 45–63, 2003.

[49] G. S. Chirikjian and J. W. Burdick, “A modal approach to hyper-redundant manipulator kinematics,” *IEEE Transaction Robot. Automation*, vol. 10, no. 3, pp. 343–353, Jun. 1994.

[50] R. J. Webster III, J. M. Romano, and N. J. Cowan, “Mechanics of precurved-tube continuum robots,” *IEEE Trans. Robot.*, vol. 25, no. 1, pp. 67–78, Feb. 2009.

[51] P. Sears and P. Dupont, “A steerable needle technology using curved concentric tubes,” in *Proc. IEEE/RSJ Int. Conf. Intell. Robot. Syst.*, 2006, pp. 2850–2856.

[52] R. J. Webster III and B. A. Jones, “Design and kinematic modeling of constant curvature continuum Robots: A review,” *Int. J. Robot. Res.*, vol. 29, no. 13, pp. 1661–1683, 2010.